PALEOENVIRONMENTAL HISTORY OF OTJIMARURU PAN, NAMIBIA, BASED ON OSL DATING AND SEDIMENT CHARACTERISTICS OF ASSOCIATED LUNETTE AND LINEAR DUNES

by

CHRISTOPHER J PLOETZ

(Under the Direction of George A. Brook)

ABSTRACT

In July of 2009 a study was undertaken at Otjimaruru pan and its associated dunes in the southern Kalahari of Namibia to understand the nature and origin of pans and lunettes. Four dune features associated with the pan were augered to depth for sediment, Magnetic Susceptibility (MS), and Luminesces data collection. The results indicate the pan-lunette systems of the Southern Kalahari originated prior to 80ka. Rapid accumulation of dunes at Otjimaruru during OIS 2 and 4 suggest that the climate was possibly dryer and the winds were stronger at this time. MS data from the dunes appear to record shifts from wet to dry climates with MS peaking during wet, stable periods, when weak soil formation was possible. The higher-resolution MS data correlate well with records from regional climate and Antarctic ice core data indicating that despite bioturbation pan-lunette complexes can be useful in paleoclimate research in the Sothern Kalahari.

INDEX WORDS: Pan, Lunette, Kalahari, Paleoclimate, OSL, Magnetic Susceptibility

PALEOENVIRONMENTAL HISTORY OF OTJIMARURU PAN, NAMIBIA, BASED ON OSL DATING AND SEDIMENT CHARACTERISTICS OF ASSOCIATED LUNETTE AND LINEAR DUNES

by

CHRISTOPHER J PLOETZ

BA, Auburn University, 2007

A Thesis Submitted to the Graduate Faculty of The University of Georgia in Partial Fulfillment of the Requirements for the Degree

MASTERS OF SCIENCE

ATHENS, GEORGIA

2011

PALEOENVIRONMENTAL HISTORY OF OTJIMARURU PAN, NAMIBIA, BASED ON OSL DATING AND SEDIMENT CHARACTERISTICS OF ASSOCIATED LUNETTE AND LINEAR DUNES

by

CHRISTOPHER J PLOETZ

Major Professor: George A. Brook

Committee: David S. Leigh
Thomas R. Jordan

Electronic Version Approved:

Maureen Grasso
Dean of the Graduate School
The University of Georgia
August 2011

DEDICATION

I am dedicating this Thesis to my Mother who never let me give up, my Father who has always supported me in everything that I do, and my sister who is always there when I need her.

ACKNOWLEDGEMENTS

There are a number of individuals who I owe a great deal of thanks. This entire Thesis would not have been possible without the assistance, guidance, and patience of my advisor Dr. George A. Brook. I am also very grateful to Eugene Marais for allowing me to stay in his home in Namibia and for all the assistance he provided in the field during my time there. Thanks are also due to my committee members Dr. David S. Leigh and Dr. Tommy Jordan for their advice and support throughout, Fong Brook for her work on the OSL samples, Brooks Ellwood for his work on the MS samples and ByungYun Yang for his assistance on remotely sensed imagery prior to field work.

I owe a special thank you to Jodie Guy, Audrey Hawkins, Emily Duggar, and Loretta Scott who helped get me home safely when I was stranded in Africa. My appreciations also go out to Nancy O'hare and Drew Parker for allowing me a place to stay while I was finishing the Thesis. I'd also like to thank Lixin Wang, Bradley Suther, Jake McDonald for their help with various geomorphic and data analysis techniques. For keeping me sane through my master's program I would like thank Michelle Palma, Taylor Johnson, Nick Kruscamp, Matt Miller, Matt Michelson, Jordan Lieberman, Laura Beacker, Michelle Flipo, Megan Freeman, Graham Pickren, Sergio Bernardes, Woo Jang, Hunter Allen, Theresa Andersen, Myron Petro, Jason Meadows, Dustin Menhart, Thomas Vanderhorst, and the countless other fellow graduate students for all the help, advice, and friendship they have given over the years. Most importantly I would like to thank the entire UGA Geography Department for being my extended family these past years and for giving me a place I will never forget. Thank you!

TABLE OF CONTENTS

LIST OF TABLES

Page

LIST OF FIGURES

Page

CHAPTER 1

INTRODUCTION

The Kalahari Desert

The Mega Kalahari is a large (ca. 2.5 million km^2) basin of windblown sand located in Southern Africa (Thomas 1997). It extends from the Orange River in the south to the southern part of the Democratic Republic of the Congo in the north (Fig. 1.1). The southern half of this region, the Kalahari Desert, has low rainfall and porous, sandy substrate. It is often described as a semi-arid thirst land as rainfall is too high for it to be classified as a true desert (Leistner and Werger 1973). The core of the Mega Kalahari basin, referred to simple as the Kalahari, comprises eastern Namibia from the Orange River to southern Angola and the eastern half of Botswana; the desert extends NNE into southern Zimbabwe and Zambia (Fig. 1.1)

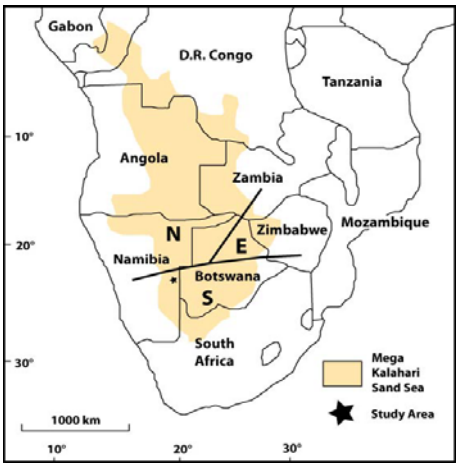

Fig. 1.1 Map of Southern Africa showing the extent of the Mega Kalahari, the location of the Northern (N), Eastern (E), and Southern (S) dune field divisions, and the location of Otjimaruru Pan (modified from Thomas and Shaw (1991).

The Kalahari lies within the summer rainfall zone of Southern Africa and is influenced by the seasonal interaction between the subtropical high-pressure cells and the Intertropical Convergence Zone (ITCZ), which creates a period of monsoonal rainfall during part of the year (Tyson and Preston-Whyte 2000). The southern Kalahari, located from 23° to 29°S is the driest part of the Kalahari with the mean annual rainfall varying between 150-200mm (Thomas and Leason 2005). In contrast, the northern part of the Kalahari in Namibia and Botswana receives up to 600-800mm of annual rainfall (Lancaster 1981, Chase and Meadows 2007) (Fig 1.2).

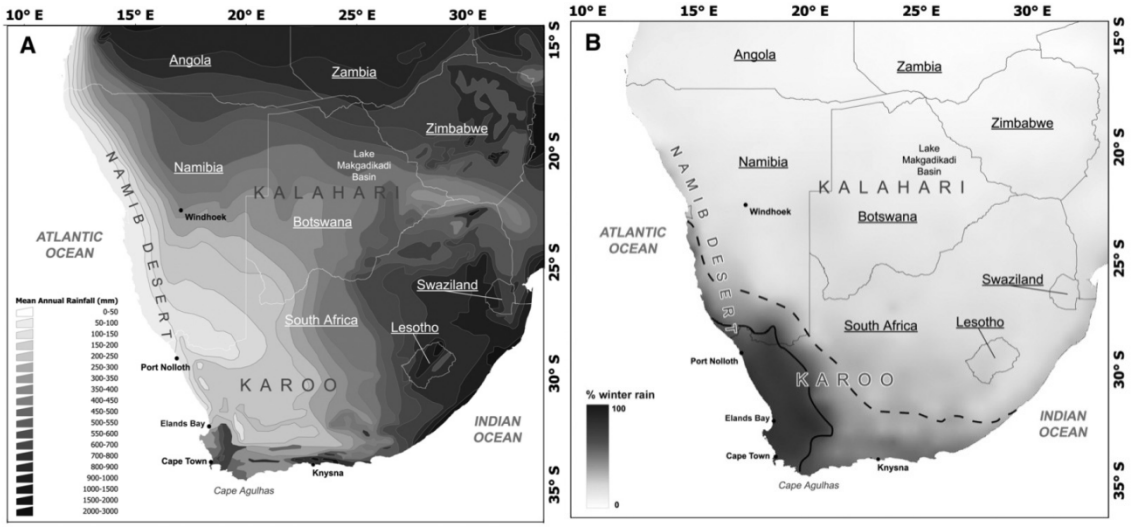

Fig. 1.2 Mean annual precipitation over southern Africa (A), and the present extent of the winter rainfall (WR), year round rainfall (YR), and summer rainfall (SR) zones (B). The solid and dashed lines mark the boundaries of the WR and SR zones respectively (Chase and Meadows 2007)

Throughout much of the year the climate of Southern Africa is dominated by the South Atlantic Anticyclone that produces a southwesterly airflow over the western section of the subcontinent (Fig. 1.3). In winter the South African Anticyclone gains strength and migrates northward as it intensifies and increases in size. In the summer months it moves south as it weakens and its more southerly position allows moist Indian Ocean air to penetrate the subcontinent bringing monsoonal rainfall (Chase and Thomas 2007).

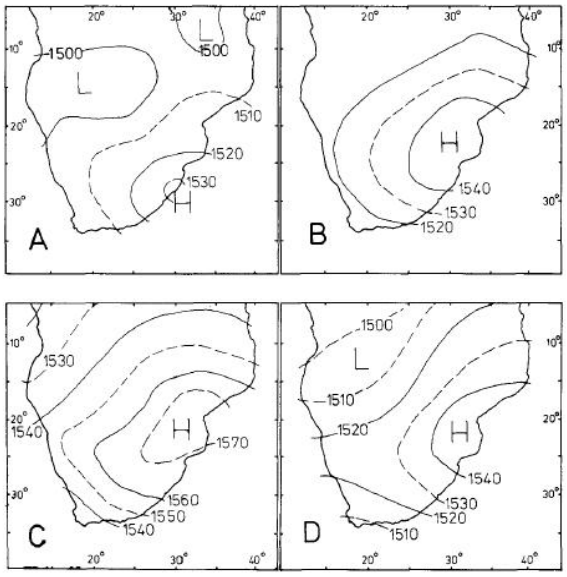

Fig. 1.3 Seasonal changes in the distribution of atmospheric pressure over Southern Africa caused by anticyclone activity. A: January; B: April; C: July; D: October. Isolines are heights of the 850 mb surface in m.(Lancaster 1981)

The Kalahari has long been known to harbor evidence for past climates markedly different from those of today (Grove 1969, Lancaster 1981). However, like most semiarid areas, and in contrast to more temperate locations, Southern Africa, and the Kalahari in particular, lacks robust dateable paleoclimate proxies such as pollen and diatoms (Thomas and Shaw 2002). The most prominent evidence of these past climate conditions is preserved in ancient dunes and dry lake basins.

The Kalahari is dominated by fields of relict, mostly linear dunes. There are three main subsystems: Northern (N), Southern (S), and Eastern (E), which have been delineated based on dune orientation and location (Lancaster 1981). Within these extensive dune fields, particularly the Southern field, there are small enclosed depressions known as pans that may have one or more crescent shaped dunes, known as lunettes, on the leeward margin. In the southern Kalahari these lunettes are generally oriented NW-SE (Lancaster 1981). They are so numerous that Lancaster (1978) remarks that "The principal geomorphic features of the Southern Kalahari are

the thousand or so pans." The largest numbers of pans are in central-southern Namibia and southern Botswana in an area known as the pan belt. In addition, within the dune fields there are several large lake basins that are largely dry today. These include Etosha Pan in northern Namibia, and Makgadikgadi Pan in NW Botswana. To the southwest and east of the Okavango River Delta are two more large lake basins, Lake Ngami, and the Mababe Depression. In the past these four lake basins contained huge lakes in stark contrast to their dry, dusty state today.

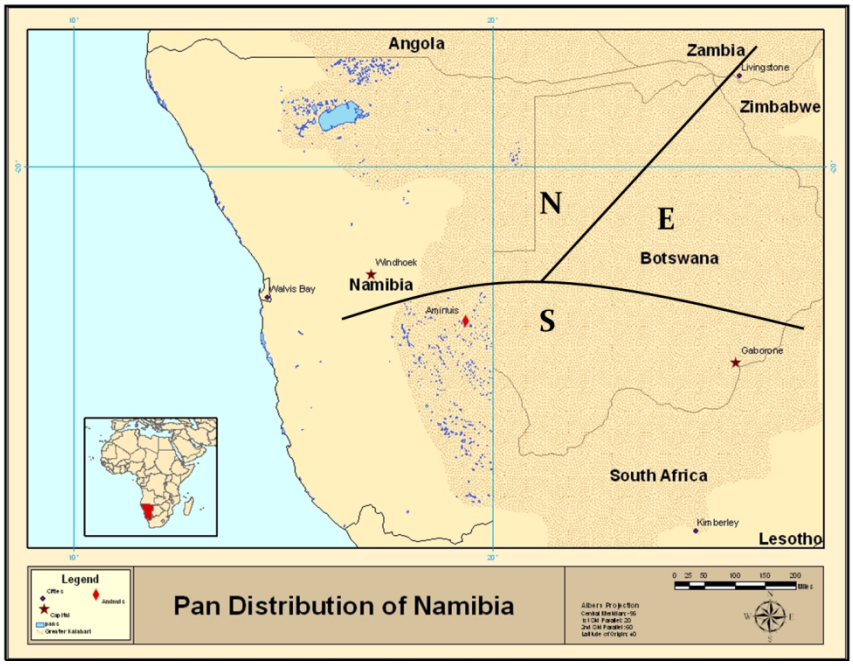

Fig. 1.4 Distribution of pans in Namibia illustrating the high concentration of small pans (blue) in the southern Kalahari known as the pan belt and the dune boundaries.

The relict dunes and dry lake basins are convincing evidence of drier and wetter conditions in the past relative to the present climate regime. The relict linear dunes (Fig. 1.5) represent a drier windier phase when conditions were more favorable to dune growth and accumulation. At present dunes in many areas are stabilized by vegetation. The paleolake basins and pans record time periods that were wetter than present when the depressions may have contained more permanent water bodies. This thesis will examine the paleoclimate evidence

from the two most dominant long-term climate proxies in the region, pans and dunes. This will be accomplished by looking at a linear dune/pan/lunette complex to uncover evidence of past climates by examining the origin and evolution of the complex itself.

Fig. 1.5 Vegetated relict linear dunes in the southern Kalahari. Note that the crests of some dunes are active due to overgrazing.

The Relict Dunes

Dune Fields of the Kalahari

Lancaster (1981) identified two linear dune fields in the Kalahari, namely the Northern Dune Field, which he divided into subgroups A and B, and the Southern Dune Field (Fig.1.6a,b). The A and B subgroups of the Northern Dune Field were later classified as separate fields by Thomas and Shaw (1990), who referred to them as the Northern and Eastern dune fields, respectively.

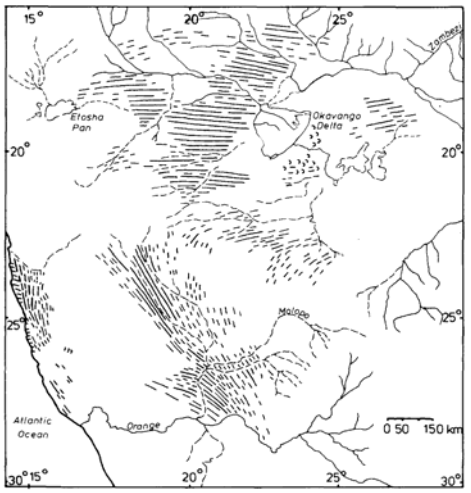

A

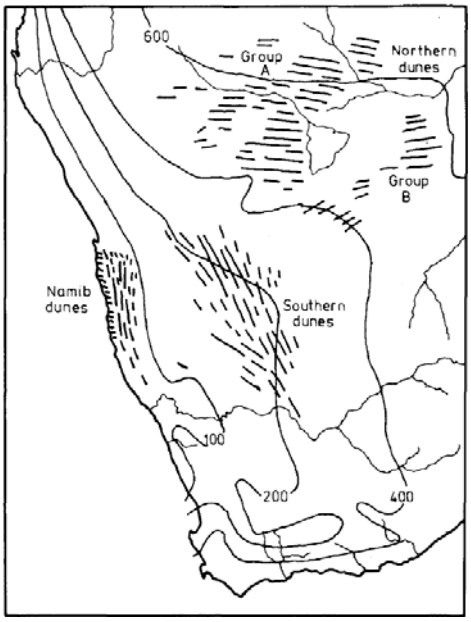

B

Fig. 1.6 Dune systems and dune fields in Southern Africa. (A) Map of the dunes compiled from LANDSAT (ERTS) imagery. (B) Relationship of fixed and active dunes to mean annual rainfall and the three dune fields (Lancaster 1981). Isohyets are in mm/yr.

The Northern Dune Field is located north of 23°S and is bounded by Etosha Pan to the west and the Okavango Delta to the east. It consists primarily of linear dunes trending WNW-ESE to WSW-ENE (Lancaster 1981, O'Connor and Thomas 1999). The linear dunes are up to 25 meters high and may continue for nearly 200km. Lancaster (1981) says they are “clearly formed by easterly winds. The Eastern system (sometimes referred to as the group B Northern Dunes or NE

dunes) is also located north of 23°S. The linear dunes of this dune field form a counterclockwise arching pattern that becomes more pronounced to the west where it finally blends into the Southern Dunes. The Eastern Dunes are often severely degraded because the present annual precipitation is 600-800 mm. In addition, because of the relatively high rainfall the dunes often have a cover of savanna woodland that further stabilizes them.

The Southern Dune Field extends from 23° to 29°S and occupies the driest part of the modern Kalahari, receiving a mean annual rainfall of 150-200 mm (Thomas and Leason 2005). This dune field is dominated by linear dunes that trend NE-SW. The majority of small pans with lunettes are located within the Southern Dune Field. The Southern Dunes are not as heavily vegetated as those in the Northern or Eastern Dune fields but are well preserved. They occur where annual precipitation is near the precipitation threshold for dune activation (Lancaster 1981), which suggests that a slight drying of the environment could potentially reactivate them. In fact, although the dunes are considered to be inactive, where vegetation cover has been removed due to overgrazing, the crests have been reactivated (Lancaster 1981).

Possible Relationship between the Three Dune Fields and the Location of the South African Anticyclone

The limits of active dunes in modern deserts are believed to be related to annual rainfall, although vegetation cover is also a factor. Lancaster (1981) has argued that 100 mm mean annual rainfall may be the threshold for dune activation. If correct, this would indicate a substantial migration of the 100 mm isohyet in southern Africa from its present position to explain the distribution of the relict dunes. It would also indicate that a slight reduction in annual rainfall could reactivate the linear dunes in the south (Lancaster 1981). These dunes are not fully active

today because the specific climate conditions necessary for dune construction are not present. Their existence, however, implies that at some point in the past the climate conditions of the region were more favorable for dune development and activity.

In the present climate regime the South Atlantic Anticyclone, normally centered on 10° E 30° S, weakens and moves southwest during the austral winter months. Although its location may shift during the year it maintains consistent southwesterly winds into western Namibia (Fig. 1.3.) (Lancaster 1981). The South African Anticyclone is much more variable in terms of its size, shape, location, and strength though the year. During the winter months it strengthens and moves northward into eastern Gauteng Province. During the summer months the South African Anticyclone retreats southward and weakens, allowing the invasion of moist air from the Indian Ocean resulting in monsoonal rainfall in the interior of the Kalahari (Lancaster 1981).

Due to fluctuations in strength between the South Atlantic and South African anticyclones, the wind direction changes seasonally (Fig. 1.7). This has a substantial effect on the transport of sand (sand flow) and the formation of aeolian features. Seasonal changes in pressure gradient affect the strength of the wind and thus the sand flow. Lancaster (1981) has shown that winter and spring winds produce the greatest sand movement. Although seasonal sand flow directions are different and seasonal changes in the sand flow direction do occur, generally they maintain a consistent directional flow (Lancaster 1981).This migration of the pressure systems is the key to understanding past climates.

During periods of increased aridity it is reasonable to assume that the South African Anticyclone was stronger and prevented the influx of moisture into the Kalahari. In contrast, when the South Atlantic Anticyclone was weaker the subcontinent was under the influence of the South African Anticyclone for a longer period of time. Alternatively, a weaker South African

Anticyclone and a stronger South Atlantic Anticyclone would have brought an overall influx of moisture to the Southern African subcontinent resulting in a wetter climate (Lancaster 1981). Increased penetration of frontal systems associated with mid latitude cyclones best explain the wetter periods recorded in many areas while the increased persistence and strength of the South African Anticyclone explains arid periods. The patterns of the relict dune fields indicate that each formed when the resultant annual circulation pattern resembled the modern winter or spring pattern (Thomas 1984).

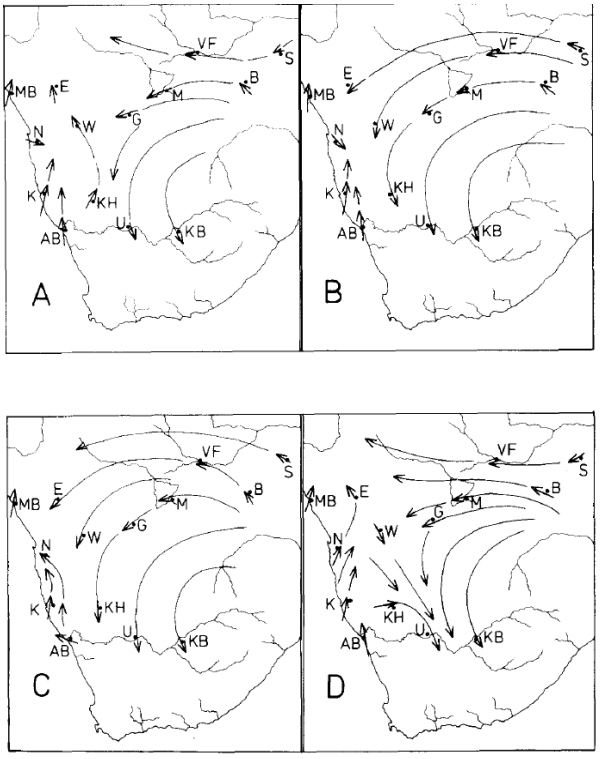

Fig.1.7 Seasonal changes in patterns of resultant sandflow in southern Africa: A. January; B. April; C. July; D. October (after Lancaster 1981)

Historical Stages in the Development of a Chronology for the Kalahari Dunes

There have perhaps been three distinct phases of research on the paleoenvironmental implications of dunes in Southern Africa since the 1970s. Phase 1 began prior to the 1990s before the application of optically stimulated luminescence (OSL) dating techniques to desert

dunes. Without reliable ways to date the dune systems, research focused on using remote observation of the earth to provide detailed imagery of the extensive dune systems in the Kalahari (Bullard et al. 1997). For example, Lancaster (1981) and others examined the alignments of the linear dunes in the different dune fields of the Kalahari to infer relative ages for each. In addition, radiocarbon ages for some dunes were obtained by dating calcrete within the dune sands (Lancaster 1990, Lancaster 1989, Lancaster 1981).

Lancaster assumed that each group of dunes represented a different period of dune formation because of the unique wind pattern that must have formed them. He determined that there were three periods of dune building during the Quaternary. The oldest period, which formed the group A (Northern) Dune Field, was believed to be sometime around 38,000 BP, based on known ages of fluvial and lacustrine features crosscutting the dunes. The Group B (Eastern) Dune Field and outer lunette dunes in pan/lunette complexes were thought to correspond to the LGM, at around 18,000 BP. The last phase of dune formation was believed to occur sometime after 12,000 BP and formed the Southern Dunes and inner lunettes of the pan/lunette complexes.

The second phase of research on the dunes began in the early 1990s with the advent of OSL dating. In the period following the first us of OSL techniques to date Kalahari dunes, more than 219 ages have been published (Chase and Brewer 2009). An example of research during this second phase is that of Stokes et al. (1998) who dug pits to a depth of 2 meters at 12 locations in the Northern Dune Field in southern Zimbabwe. This work revealed four phases of aridity at 95-115, 41-46, 20-26, and post 20 ka. At the time this was the only and oldest chronology of dune building ever documented. In contrast to these older ages, a series of 2 meter deep pits dug in the Southern Dune field revealed only two phases of aridity at 10-17 ka and 23-28 ka(Stokes and

Thomas 1997). These studies led to the incorrect assumption that the Northern Dunes were older than the Southern Dunes. The reason the OSL ages suggested this is because the depth of pits dug into the dunes for sampling was only 2 meters. In the Northern Dunes sampling to two meters was sufficient to encounter very old dune sand (e.g. 115ka). In contrast, in the southern and Eastern Dunes the sand at 2 m depth was relatively young, only dating back to around 45 ka.

During the third phase of research in the Kalahari, efforts were made to recover dune sand from greater depth. Because of this it has been discovered that the Southern Dunes do in fact date back to the same time as the Northern Dunes, and in fact record a number of events not shown in the records from the Northern Dune Field (Stone and Thomas 2008).

(Thomas and Shaw 2002) compiled the available ages for linear dunes in the Kalahari using frequency histograms (Fig.1.8.). This revealed six phases of dune activity. In the southern interior dune building episodes were defined at ca. 30-23, 16-10, and 8-17.5ka. In the Central and Northern Kalahari three phases of dune building were recognized at ca. 115-95, 46-41, and 26-20ka.

Recent research in the southern Kalahari, has attempted to extend the record of dune development by dating deeper sediments. For example, (Telfer and Thomas)augered8 linear dune sites in the Witpan area in South Africa to depths up to 15 meters at 0.5 meter intervals. The reported OSL dates indicate periods of aridity at 9-15, 19-21, 27-35, 52-57, 76-77, and 95-105 ka demonstrating that the Southern Dunes are in fact of a very similar age to the Northern Dunes and record several more building episodes. It is for this reason that the most recent phase of study has been focused on extending the record in the south and refining the interpretation of the OSL ages. It is because of these efforts that the vast majority of the OSL dates (140) have come from the Southern Dune Field.

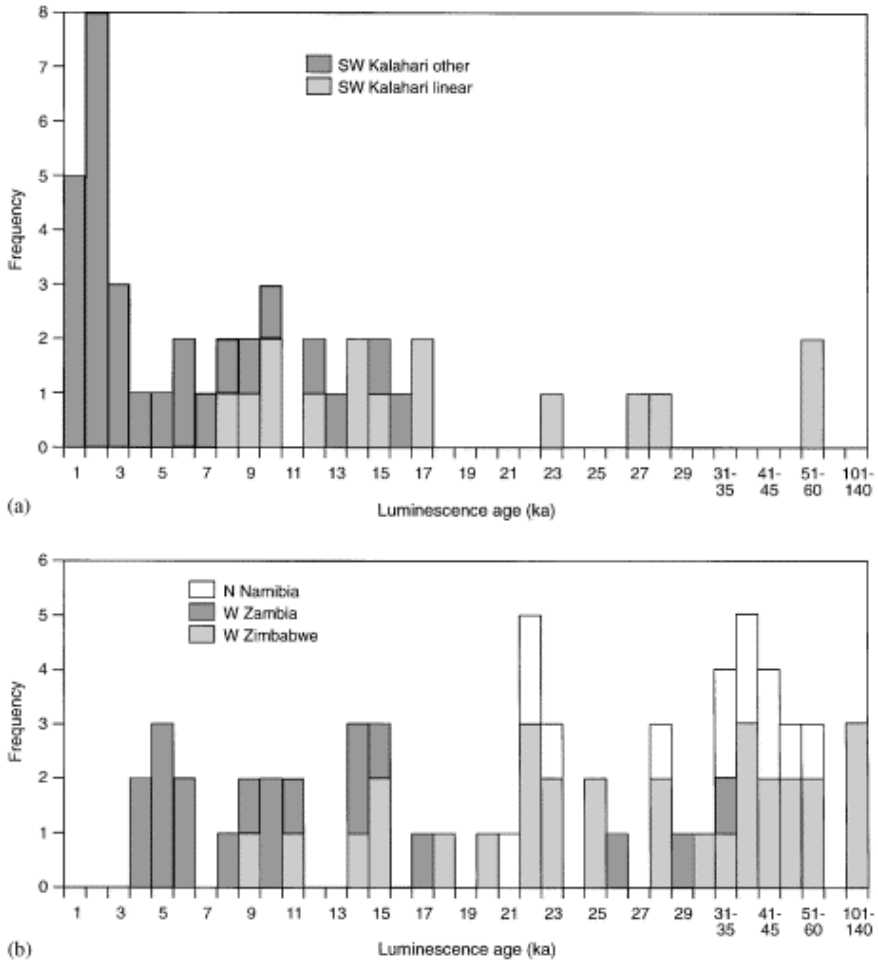

Fig. 1.8 Histograms of dune and aeolian sediment luminescence ages derived from (a) the southern Kalahari and (b) the middle and northern Kalahari. Central points on ages are plotted without the inclusion of 1 sigma deviations. The latter have been used to assess age clusters and to assess the probability of peaks of aeolian deposition within the record. Taken from (Thomas and Shaw 2002).

Problems Interpreting Dune OSL Ages in Paleoclimate Terms

The accumulation of the ancient Kalahari dune fields appears to have been episodic, with long periods of stability punctuated by brief episodes of extreme climate when the dunes were formed. Present-day aeolian activity in the Kalahari region is complex. Dunes with mobile sediment along overgrazed, poorly-vegetated crests are very common in the Southern Dune Field in particular. It remains unclear how best to interpret the OSL age data. Most commonly,

researchers consider the ages to be evidence of dune building periods. However, it is also possible that they record periods of dune stability or degradation when bioturbation, which is an important process in the Kalahari, would result in the bleaching of sands in the upper 0.5-1.5 m of the dune. In fact, Bateman et al. (2003) noted that when viewing the complete dune record of the Kalahari there appear to be no discernable breaks in age that might help to identify climatic shifts from wetter to drier or vice versa.

Another problem in the use of dune systems as paleoenvironmental indicators relates to what controls dune activity. (Chase 2009) has argued that the Kalahari dune systems are primarily wind rather than precipitation limited. Assuming a Last Glacial Maximum wind speed 117% of present and the same precipitation, he reports that only this slight increase in wind speed would be needed to reactivate the southern linear dunes. This calls into question exactly what is being recorded in the dune ages and their use as proxies for greater aridity in the past. Chase and Brewer (2009) have also noted that dunes may only preserve sediments deposited during the early parts of arid phases, owing to the potential for the reworking by the wind of upper sediments during the onset on a subsequent phase of dune activity. In essence, there is a growing awareness that the paleoclimatic significance of sand accumulation on dunes may be complex and must be better understood. This involves the recognition that aeolian accumulation may not always relate solely to aridity. This was recognized by Lancaster who developed a mobility index: $M = W(P/PE)$, where W is the percentage of time the wind is above a threshold to transport sand, P is precipitation and PE is potential evapotranspiration (Lancaster 1989).

The Ancient Lake Basins

The shorelines of paleolakes (Fig. 1.9.) have long been recognized as paleoclimate proxies for much wetter phases of climate in the past (Grove 1969). A compilation of the available age data for the largest paleolakes in the Makgadikgadi, Ngami, and Mababe basins is illustrated in Figure 1.10. High stands of a massive paleolake, Lake Thamalakane, which linked the Ngami and Mababe basins in Botswana with the Okavango Delta and Zambezi River system were radiocarbon dated to 17,000-12,000 ^{14}C yr BP (Thomas and Shaw 2002). Thomas and Shaw (2002) also report radiocarbon ages of 40,000-35,000 ^{14}C yr BP for a lake high stand in the Makgadikgadi basin in northern Botswana. Burrough et al. (2009b) examined relict shorelines and beach ridges around the Makgadikgadi basin dating high lake phases by OSL to 8.5 ± 0.2, 17.1 ± 1.6, 26.8 ± 1.2, 38.7 ± 1.8, 64.2 ± 2.0, 92.2 ± 1.5, and 104.6 ± 3.1 ka. Studies of shorelines along the western margin of Etosha Pan in northern Namibia suggest four periods of increased wetness during the Holocene at 13, 7–5, 4.5–3.5, 2.5–1.7 and ca. 1.0 ka with the oldest period being a prominent and widespread interval of wetness (Brook et al. 2007).

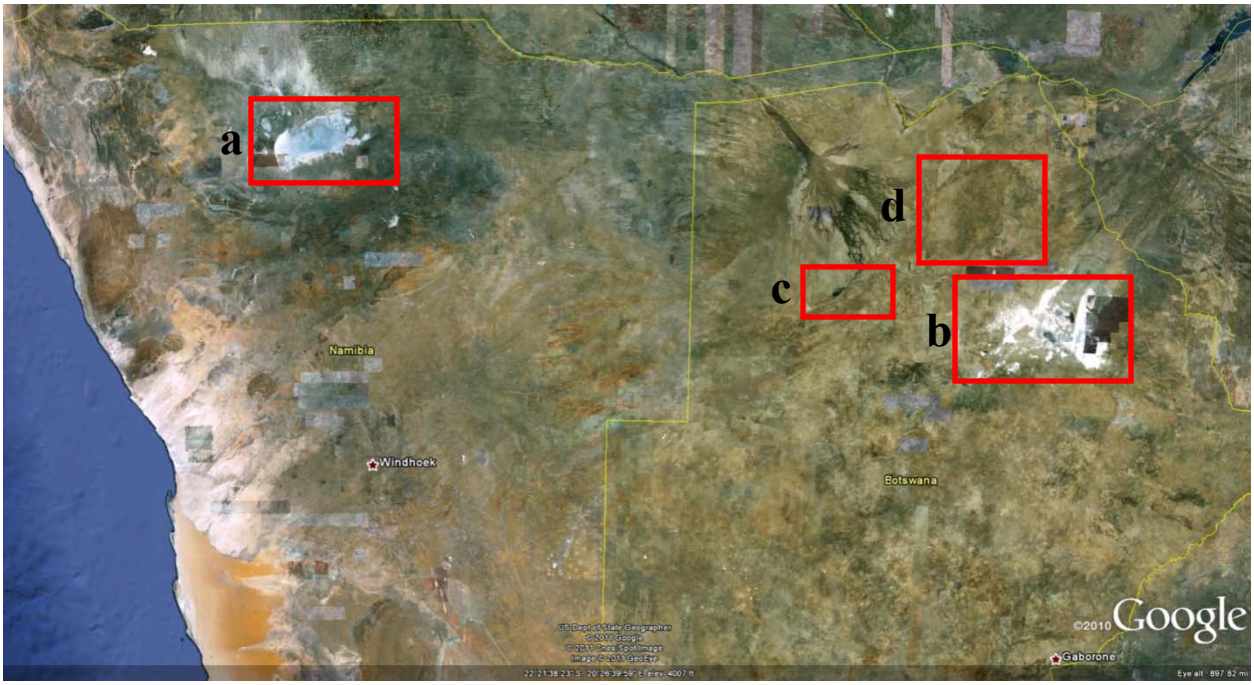

Fig. 1.9 Satellite imagery from Google Earth showing the large paleolake basins of Southern Africa: A) Etosha, B) Makgadikgadi, C) Ngami, and D) the Mababe Depression.

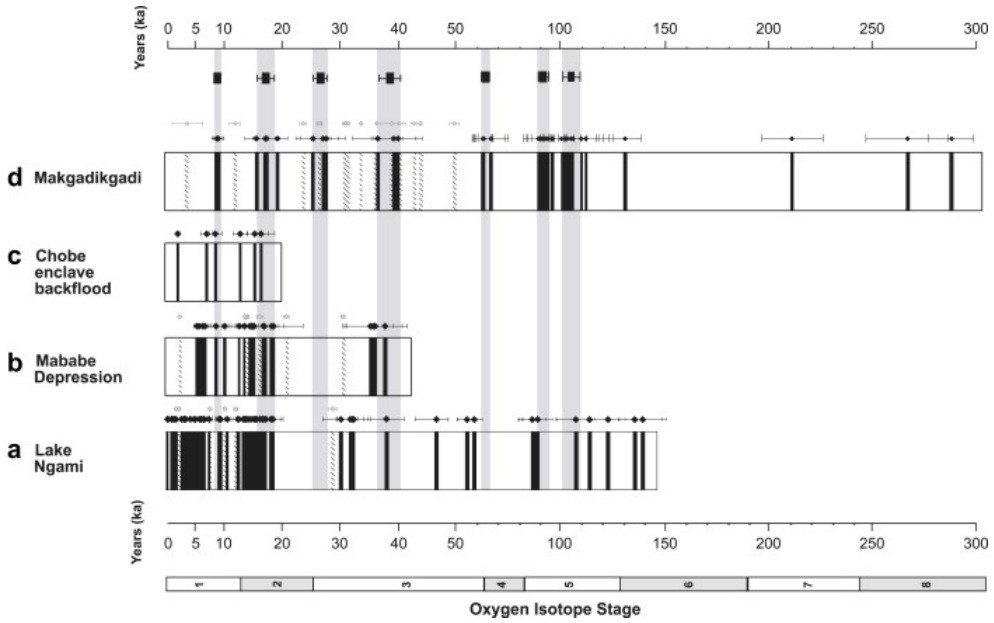

Fig. 1.10 High lake stands in the Makgadikgadi, Ngami, Mbabe basins and in the Chobe enclave. Inferred paleo-mega-lake phases are shaded in grey. Black bars within rows refer to dated shoreline ridge accumulation periods. Actual dates with uncertainties (1 standard error) are plotted adjacent to these columns in black. Hatched bars indicate dated periods of calcrete formation within the basins and shorelines, the ages and associated errors are shown adjacent to these columns in grey. Figure from (Burrough, Thomas and Bailey 2009a).

Limited work has been conducted on pan/lunette systems in the southern Kalahari. OSL ages for pan floor sediments at Witpan, in southern Namibia, suggest wetter intervals at ca 20 ka and 32 ka. Luminescence ages for lunettes at Witpan ranged from 1.1–1.5 ka and 17 - 11 ka(Telfer and Thomas 2006). Lawson and Thomas (2002) dated sediments at several Southern African pans and found numerous phases of sediment deposition in the lunettes over the past 18 ka and not always synchronous with postulated phases of linear dune accumulation (Chase 2009). Lawson and Thomas (2002) conclude that sedimentation on lunette dunes is controlled by a range of factors not necessarily connected to regional aridity. They also note that the paleoenvironmental interpretation of lunette ages is problematic because not enough is known about the conditions that lead to the formation of lunettes.

Pan-lunette Systems

Closed basins known as pans are a common feature in the Southern Kalahari Desert (Fig. 1.11.). In places they constitute up to 20% of the surface area and can range in size from a few meters to tens of kilometers across (Goudie and Wells 1995).During the summer wet season pans may be occupied by ephemeral lakes while in the dry season their floors may be covered with a layer of precipitated salt. Many pans are in areas of closely-spaced linear dunes and some may have one or more dunes, or lunettes, on their downwind sides.

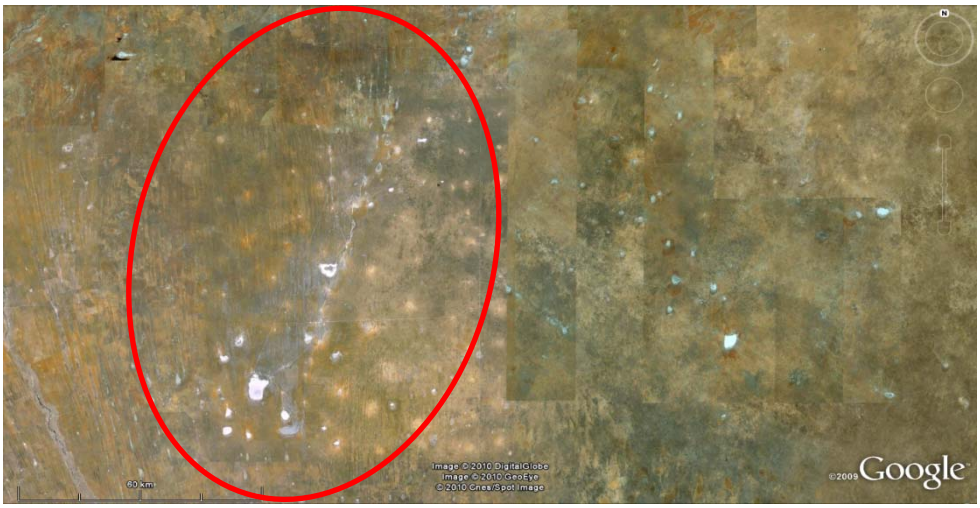

Fig. 1.11 Satellite image showing pans in the area around Otjimaruru Pan, Kalahari Desert.

Lunette dunes can be identified by their distinctive crescent shape for which the term lunette is derived (Lawson and Thomas 2002). Lunettes may come in multiples and may vary in color and orientation depending on the prevailing wind direction. The outer dune is usually an orange-red color similar to the overlying Kalahari sand. The red color is normally due to the high iron content of the sands. The inner dune/s range from light brown to white yellow, the latter being correlated to a higher sulfur content (Marker and Holmes 1995).

Lunette dunes have been described as accumulations of sediments deflated from dry lake floors during periods of aridity (Fig. 1.12) (Holmes et al. 2008, Lancaster 1989, Lawson and Thomas 2002). Variables thought to be responsible for sediment deflation from the pan floor and the creation of lunettes include the pan width, orientation, underlying lithology, and perhaps most important, a low or fluctuating water table (Thomas et al. 1993). By this model of formation, luminescence ages from a depositional unit of a lunette's stratigraphy are considered to reflect a period of aridity.

In Australia however, lunettes fringing some pans have been described as accumulations of deflated sediments deposited initially by wave action as beach ridges (Fig.1.13) during periods of high lake-level (Chen 1995). In this scenario lunette dune ages document periods of greater precipitation and not aridity as in the hypothesis discussed earlier.

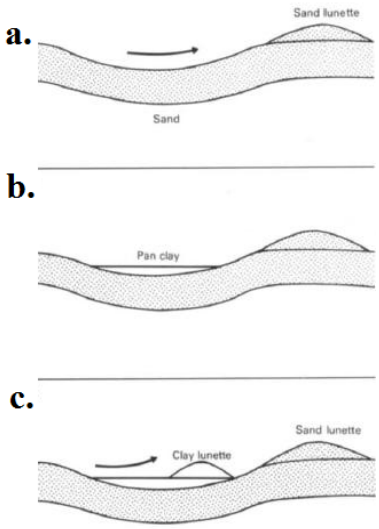

Fig.1.12 Formation of lunette dunes by deflation of pan sediments: a) during a dry period a deflation hollow is formed, b) the water table rises and a small lake develops, c) the water table drops again deflating pan floor sediments into a secondary lunette.

Investigators working on Lake Victoria sought to characterize its hydrological conditions based on the sedimentology of its lunette dune deposits. They determined that the non-clay lunettes are the result of deflated sand-sized shoreline deposits that are mobilized and transported by wind action (Chen 1995). According to Marker and Holmes (1995) lunettes in the Kalahari are formed through sediment weathering of the pan floor during periods of high groundwater level and then transported by wind to the lunette. Lunettes are also derived from sand transported over the dry pan floor to the lunette from upwind linear dunes. If true, then the resulting lunette would have a similar grain size distribution and chemical composition to the Kalahari linear dune sands, and record ages that correlate with known dry events. The distinct color differences

between the outer and inner lunettes are not explained by this model of lunette development in Southern Africa. Alternative models will be examined thoroughly in this study. It should be noted that unlike the Australian clay dunes, the lunettes of Southern Africa are primarily composed of sand and do not form through the clay pellet theory as described by Bowler (1973). Lunettes in the Kalahari appear to have a grain size distribution more similar to the wave-deposited beach ridges (Fig. 1.10) of the much larger lakes in Australia (Chen 1995). This raises some intriguing questions regarding the interpretation of luminescence data acquired from these features.

Fig. 1.13 Wave action at Etosha pan Namibia.

Thesis Aim and Objectives

The aim of this research is to examine the origin and environmental history of the Otjimaruru Pan/lunette system in the southern Kalahari of Namibia. To achieve this aim, the research has a number of specific objectives.

Objectives:

1) Identify and map the landforms at Otjimaruru Pan, including pan floor features, lunette dunes, beach ridges, and linear dunes.

2) Analyze and compare the sediment characteristics [e.g. texture, color, magnetic susceptibility (MS), salt content and chemical composition] of the linear and lunette dunes at Otjimaruru in order to understand the processes that may have formed them.

3) Develop and compare chronologies for the accumulation of the linear and lunette dunes using OSL dating to document periods of increased or reduced accumulation. Previous work on nearby Aminuis Pan has documented lunette deposition to 168 ka (Brook et al. pers. comm. 2010).

4) Synthesize the sediment, age, and morphological data for Otjimaruru Pan to establish a model for the origin and subsequent evolution of Otjimaruru Pan and other pan/lunette systems in the region. In particular examine whether the lunette systems were formed predominantly during arid (entirely aeolian) or humid (water transported and then moved by wind) intervals.

5) Develop a paleoclimatic history for Otjimaruru Pan using the age and sediment data (particularly high resolution MS data) for the period of record and compare this with regional and global records of climate change.

The Study Area: Otjimaruru Pan

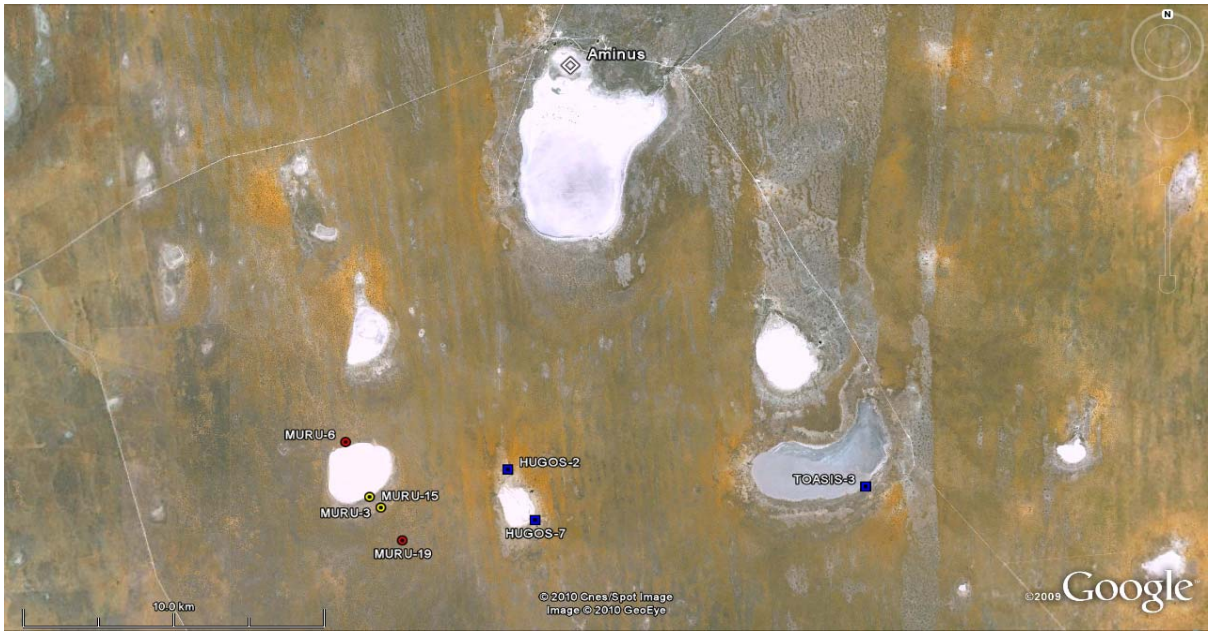

Fig. 1.14 Map of the study area showing auger sites (circles) and sampled wells (squares). Circle color depicts relative sediment color.

Otjimaruru Pan (Fig. 1.14) centered at 23° 47′ 32.62″ S, 19°18′ 25.59″ E in Namibia is one of numerous circular to oval depressions in the Southern Kalahari Desert (Lancaster 1989). The pan is located 265 km SE of Windhoek in the Gobabis farming district of the Omaheke region. The pan is 2.5 km long, 2.0 km wide and has an average altitude of 1200 m.a.s.l. It is located within a field of linear dunes trending approximately N-S parallel with the predominant wind from the north. There are two prominent lunette dunes on the downwind, southern margin of the pan with limbs that extend northwards more than half the length of the pan. The lighter colored inner lunette rises about 18m above the pan floor while the darker-colored outer lunette crests more than 26 m above the pan floor. In addition to the lunettes, there is a pale-yellow, 4 m-high shore ridge around two thirds of the pan that is most prominent on the downwind margin.

Otjimaruru Pan is located in an area with a high pan concentration known as the pan belt, near the Botswana border. There has been no detailed geological survey of Otjimaruru Pan but

studies of nearby areas show that the underlying sediments range from Jurassic-modern (Fig. 1.15). Surficial sediments are mainly Quaternary aeolian sands overlying Kalahari Formation calcretes, calcareous sandstones and silcretes that date back from the Paleocene (ca. 60 ma) to the Pliocene (Singletary et al. 2003, Partridge and Maud 1987). In turn these overlie granites and gneisses that are exposed in the NE corner of Otjimaruru(Wright 1978).

The lowermost duricrusts consist of light-colored massive calcareous sandstones that may contain shatter breccias cemented by calcareous material possibly deposited from groundwater. In places the original carbonate material has been completely replaced with chalcedonic silica transported as dissolved silica in an alkali solution during a wet phase of climate (Wright 1978). The older silcretes are up to 7 m thick. The younger calcretes in the pans consist of thin soft white/grey-white deposits indicating a more recent formation (Wright 1978). Kalahari Formation sands are generally rounded to sub-angular and are likely derived from Karoo sediments and may not indicate an aeolian origin because of this (Grove 1969).

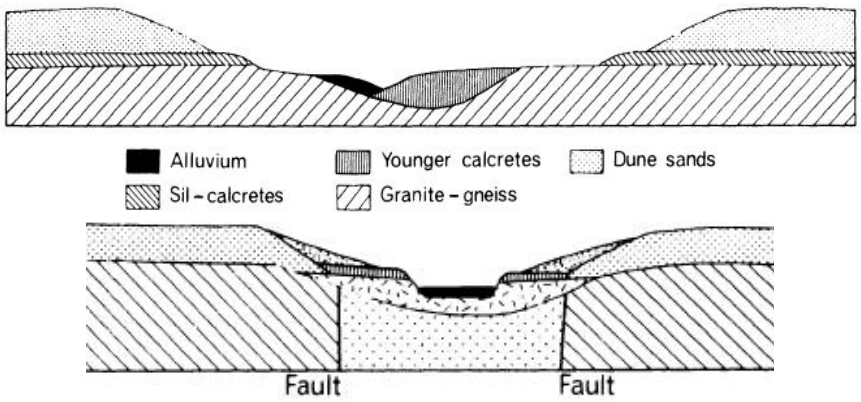

Fig. 1.15 Typical geological characteristics of pans in the Kalahari (Lancaster 1981).

Otjimaruru Pan lies within the summer rainfall zone of Southern Africa so the climate is characterized by a wet summer and a dry winter. Local precipitation is less than 200 mm a year

with 75-85% occurring in the austral summer months (Stokes et al. 1998). As mentioned previously, the climate of the region is controlled by two dominant high pressure atmospheric circulation systems: the South African and the South Atlantic Anticyclone (Fig. 1.3).

Otjimaruru Pan was selected for study because of its simple form, modest size, relative ease of access, and proximity to Aminuis Pan, which has been studied previously (Brook et al., in prep.)

Significance and Scientific Contributions

The understanding of paleoclimate in Southern Africa is important as it will provide needed information for global climate models that currently lack reliable data for the region. In a time of global warming, being able to model past and future climates is critically important. Although there are hundreds of pan/lunette systems in the Kalahari, there is very little information on their origin and subsequent evolution, particularly based on reliable chronological data. This study will provide the first detailed study of pan/lunette systems in the Kalahari and the first long record of climate change for the region based on data from such a system. By demonstrating the use of pan/lunette landforms in paleoclimate research this study will open up a new avenue of research for future studies in the region.

Thesis Outline

Chapter 2 of this thesis provides a detailed description of the methodologies employed, including site selection, sample collection, as well as the analysis of grain size, color, magnetic susceptibility (MS), and chemistry. Finally, the theory and practice of OSL dating are discussed. Chapter 3 outlines the basic results of the various analyses that were undertaken. Evidence on the

origin and evolution of pans like Otjimaruru is presented in Chapter 4 and a model of pan development is presented. Chapter 5 examines the paleoclimate record from Otjimaruru for the last ca. 80 ka and Chapter 6 compares this record with other long regional and global records. Finally, Chapter 7 summarizes the major conclusions of the research.

CHAPTER 2

METHODS

Fieldwork

Prior to fieldwork, possible pans and lunettes for study were chosen by examining Landsat 7 satellite imagery. These sites were examined on the ground before the final study site and possible augering sites in the dunes were selected. Otjimaruru Pan was selected for study and four dune locations were chosen for augering. Auger sites MURU-3 and MURU-19 are at the crests of the inner yellow and outer red-orange lunette dunes southwest of Otjimaruru Pan (Fig. 2.1). MURU-6 is located at the crest of a red-orange linear dune that intersects and terminates at the northern margin of the pan, and MURU-15 is on a hummocky, yellow shore ridge that fringes almost two-thirds of the pan perimeter. In addition to these auger sites a 110 cm vertical exposure of a cemented section of the shore ridge was cleaned and sketched and a block sample was taken from the base for possible OSL dating (Fig. 2.2).

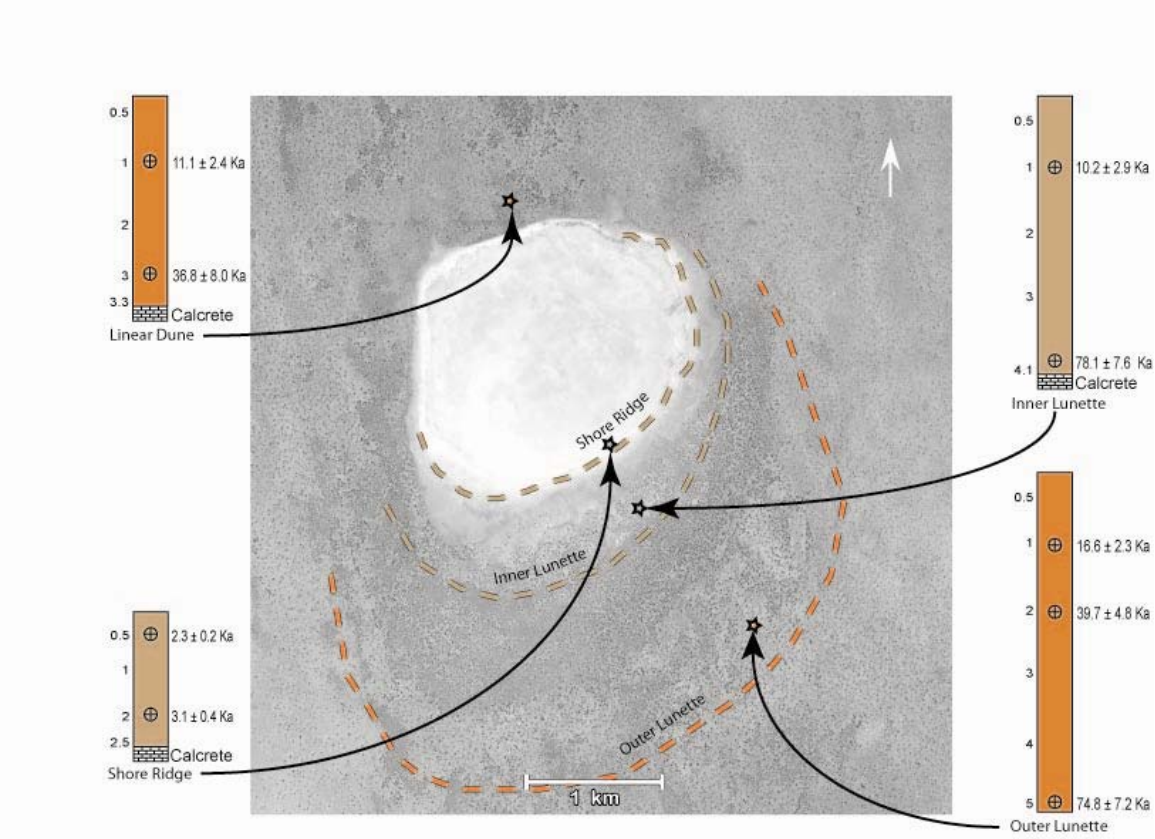

Fig. 2.1 Annotated air photo showing the location and stratigraphy of the 4 Auger sites of Otjimaruru Pan and the relative depths of the OSL samples.

Fig. 2.2 Cleaned surface of a 110 cm vertical exposure of a cemented section of hummocky yellow shore ridge sediments.

One transect was walked NW to SE from the linear dune (MURU-6) to the outer lunette (MURU-19) and a second N to S from the inner lunette (MURU-3) to the outer lunette (MURU-19) in order to ground truth the satellite imagery. Along each transect a variety of features was noted: salt crusts, calcrete formations, pan margins to the shore ridge, distinct changes in vegetation, and surface sediment texture and color. Differences in vegetation were noted to assist with the analysis of variations in spectral signature visible on the satellite imagery. Tape and GPS coordinates were used to define positions and relative distance from other features along transects.

Detailed descriptions of the auger sites were taken along with GPS coordinates. Also, depth of sediment samples from the auger sites were measured with a tape and marked on the auger tubes.

Sample Collection

At each auger site samples were collected for OSL dating and sediment analysis from the surface, 50cm depth, and then at 1 m intervals to 6 m depth, or to the maximum depth possible. When OSL samples were collected approximately 300g of sediment was also collected for grain size analysis. Smaller samples of 20-40g were collected at approximately 12 cm depth intervals (the approximate depth for recovery of one auger bucket of sediment) for MS measurements. OSL samples were obtained by inserting a tin can vertically downwards into the sand packed into the auger bucket (Fig. 2.3 and 2.4.), and then turning the auger bucket upside down to remove the can full of sand. The bottom of the can was pierced to allow air to escape as it was inserted. During augering of the inner lunette dune at MURU-3, the sand was so fine and dry that it could not be brought to the surface easily in the auger bucket. Therefore, to obtain

samples from the upper 2 m of the dune a 2 m deep pit was excavated and samples for OSL dating were obtained by hammering a PVC pipe into the wall of the trench. After collection, tops/caps were placed on the sample cans and tubes and these were sealed with duct tape and then wrapped in black plastic to shield them from sunlight.

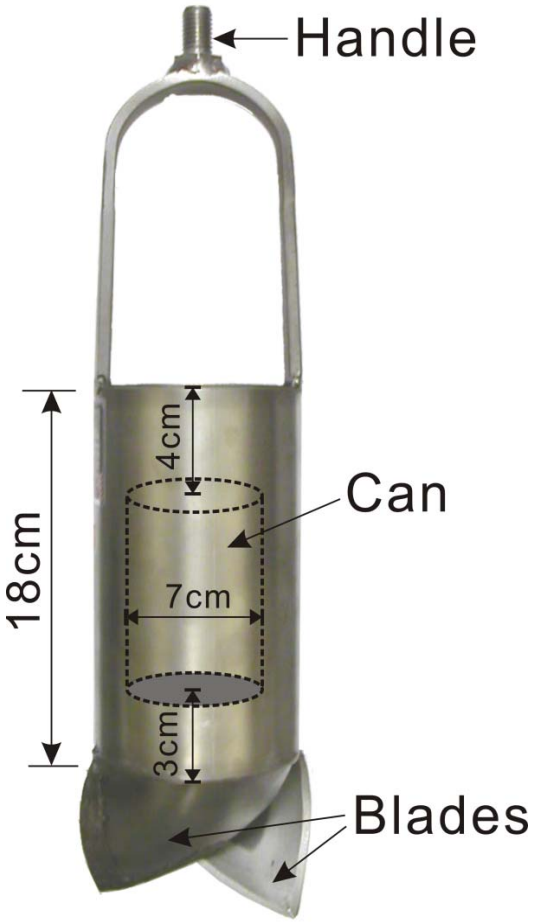

Fig. 2.3 Sand auger depicting tin can used for OSL sample collection. The top of the can is pierced to allow air to escape.

Fig. 2.4 Sand auger for sampling at 6 m depth. Collected samples are in the foreground

The original research plan was to also collect OSL and sediment samples from the pan floor and to reach groundwater to obtain samples for chemical analysis. However, this was not

possible because the pan sediments were only a thin veneer over a layer of silcrete or in places bedrock. Other pans in the area had exposures of calcrete in their floors and had natural or man-made wells in the floors or around the margins. To obtain information on the local groundwater chemistry, water samples were taken from wells at the Hugos and Taosis pans and water levels were measured relative to pan floor elevations. There are small settlements at Taosis and Hugos Pan and numerous domesticated animals use the wells (Fig. 1.11). Significantly, there are no wells or settlements at Otjimaruru Pan, possibly because the ground water table is at greater depth there. The absence of people was another reason Otjimaruru Pan was chosen for study.

Laboratory Analyses

Sediment Color and Granulometry

Dry sediment color was determined using a Munsell color chart. Sediment texture was assessed by a combination of sieving and pipette analysis (Gee 1986). Using a sample splitter, subsamples of 20-30g were taken for particle size analysis from the Otjimaruru sediment samples. Pretreatment of samples prior to analysis did not involve HCl-removal of carbonate as this would have removed much of the silt- and clay-sized carbonate material derived from the pan floor and nearby dunes. Each sample was placed in a fleaker and immersed in a solution of Sodium hexametaphosphate (50g/L) to disperse clay sized particles prior to shaking. A pipette was used to extract 25ml of suspended sediment from 5cm depth. The subsample was oven dried and weighed to determine the clay sized faction (this fraction may also include dissolved $CaCo_3$). The remainder of each sample was wet sieved to separate sand from silt and clay. The sand fraction was then dry-sieved at 0.5 phi intervals. Sediment statistics, including, mean grain size,

sorting, skewness, and kurtosis were determined using GRAVISTAT Version 6.0 (Blott and Pye 2001) and the Folk and Ward graphical method of analysis (Swan, Clague and Luternauer 1978).

Magnetic Susceptibility

MS measurements reported in this paper were made by Dr. Brooks B. Ellwood using the susceptibility bridge in the Department of Geology at LouisianaStateUniversity. The bridge was calibrated relative to mass using standard salts reported by McMichael (1992) and CRC tables. MS is reported in terms of sample mass because volume is very difficult to measure while mass is not. Meters cubed per kilogram (m3/kg) are the units after conversion of magnetic susceptibility from volume to mass the values are reported relative to a size m^3 and a mass in kilograms in SI (system international) units. The instrument is calibrated directly relative to mass while other instruments are calibrated relative to a standard volume and convert the results to mass units using estimates of density of samples introducing an error in the reported results. Because it is much easier and faster to measure with high precision than is volume, and it is now the standard for MS measurement.

Chemical Characteristics

Selected sediment samples and all well-water samples were analyzed for the 20 elements: Al, B, Ba, Ca, Cd, Co, Cr, Cu, Fe, K, Mg, Mn, Mo, Na, Ni, P, Pb, Si, Sr, and Zn using inductively coupled plasma mass spectrometry (ICPMS) at the University of Georgia Chemical Analysis Laboratory. For sediment, 5 grams of each sample was placed in a polypropylene test tube and shaken with 20 ml of dilute double acid (HC1, H_2S04) extraction liquid, and then filtered through Whatman filter paper; approximately 1 ml of the extract was analyzed. For water

samples, 5 ml from each sample was placed in a clean culture tube with a polypropylene-lined cap and 1 ml of persulfate oxidizing reagent was added. The tube was then placed in an autoclave at 19 psi for 45 min.

OSL Dating Sample Preparation and Measurement

All laboratory processes of sample preparation and luminescence measurement were carried out in a darkroom with subdued red light. Raw samples were treated with 10% HCl and 20% H2O2 to remove carbonate and organic matter. The dried samples were sieved; there were too few particles in the range 90-125 μm (recommended grain size) for dating so grains of 125~180 μm were used. Heavy liquids with densities of 2.62 g/cm3, 2.75 g/cm3 and 2.58 g/cm3 were then used to separate the quartz and feldspar fractions. Quartz grains were treated with 40% HF for 60 min to remove the outer layer irradiated by alpha particles and any remaining feldspars grains. Then, all samples were treated with 1 mol/L HCl for 10 min to remove fluorides created during the HF etching. Pure samples of quartz grains in the range 125-180 μm were acquired in this way for dating.

OSL measurements were carried out in the Luminescence Laboratory of the University of Georgia, using an automated RisøTL/OSL-DA-15 reader (Markey 1997). Light stimulation of the quartz mineral extracts was undertaken with an excitation unit containing blue light-emitting diodes (λ=470±30 nm).(BÃ¸tter Jensen 1999). Detection optics comprised two Hoya 2.5 mm thick U340 filters and a 3 mm thick Schott GG420 filter coupled to an EMI 9635 QA photomultiplier tube. Laboratory irradiation was carried out using 90Sr/90Y sources mounted within the reader, with dose rates of 0.0904 Gy/s.

The purity of quartz were checked by IRSL at 50°C and the results showed that no feldspar grains remained in any of the quartz fractions. The equivalent dose of quartz was determined by the single aliquot regenerative-dose (SAR) protocol (Murray 2000, Wintle 2006). All measurements were made at 125°C for 60 s after a pre-heat to 260°C for 10s. The pre-heat plateau test and recuperation test and dose recovery test shows the SAR protocol is reliable for the samples used in this study.

The environmental dose rate is created by the radioactive elements in the grains of the sample and in the surrounding sediments, with a small contribution from cosmic rays. For all the samples measured, a thick source Daybreak alpha counting system was used to estimate U and Th for dose rate calculation. K contents were measured by ICP90, using the sodium peroxide fusion technique at the SGS Laboratory in Toronto, Canada. All measurements were converted to alpha, beta and gamma dose rates according to the conversion factors of Aitken (1985). The dose rate from cosmic rays was calculated based on sample burial depth and the altitude of the section (Prescott 1994). All of the samples dated are aeolian so that a water content of 5±2.5% was assumed in age calculations.

CHAPTER 3

RESULTS

Sediment Characteristics

Grain size characteristics for the samples collected from the four dune auger sites are shown in Figure 3.1 (a, b, c, d) and Table 3.1. The sediment samples from all 4 sites were dominated by medium to fine sand with average mean grain size ranging from 2.98-2.25 phi. Sediment from the linear dune had the largest average mean grain size of 2.25 phi while sediment from the shore ridge had the smallest at 2.98 phi. Sand from the inner and outer lunette dunes had a mean grain size between those of the shore ridge and linear dune. The inner lunette had a mean grain size of 2.47phi and the outer lunette 2.43 phi.

Average mean grain size in phi units is lowest (coarser) in the linear dune on the upwind side of the pan and highest (finest) in the shore ridge on the downwind side. Average grain size coarsens with increasing distance downwind on the southern side of the pan. A possible explanation is that sediment from the shore ridge is incorporated into the two lunette dunes resulting in a smaller mean grain size for the latter. This would also account for the carbonate material that was found in the two lunettes and not in the linear dune.

The average percentage of very coarse and coarse sand is highest in the linear dune where it makes up nearly 10% of the total; the lunette contains the least at just over 2%. The inner lunette and shore ridge have roughly 6% very coarse and coarse sand. Medium to fine sand

constitutes almost 75% of sediment in the outer lunette and roughly 66% of the inner lunette and linear dune sediment. The shore ridge has the lowest percent of sand in this range but it still makes up 54% by weight. The shore ridge has the highest percentage of very fine sand, almost 20%. Very fine sand makes up 14-16% of the sediment in the other dunes. The average silt and clay factions are also much higher in the shore ridge than in the linear and outer lunette dune. However, the inner lunette has about the same, 5% and 8% respectively.

The percent of coarse sediment (shown in Table 3.2) at the surface and at 0.5m is higher for all dunes for almost every sediment size. In the linear dune the percent of very coarse, coarse, fine, very fine, silt, and clay sized particles increases with depth. The medium sand size particles however decreased with depth. In the outer lunette very coarse, coarse, and fine sand also increase with depth. The sand size fraction of very fine sand and silt increases with depth until 3m where it begins to decrease again. The clay fraction of the outer lunette follows a similar pattern to the other fraction sizes described above.

The inner lunette's very coarse, coarse, and medium sand fractions all increase with depth. The fine sand fraction shows a decrease with depth and the very fine sand fraction shows an increase until 2m where it begins to decrease. The silt fraction in this dune remains fairly uniform but the clay fraction sees a significant increase from around3% to nearly 10% with depth. The very coarse and coarse sand fractions of the shore ridge increase with depth while the medium sand fraction decreases with depth. The fine sand and very fine sand fractions both show an increase with depth until 2m then decrease at the base. The clay fraction of the shore ridge is high at the surface and then drops off slightly before increasing with depth.

None of the samples from the dunes was well sorted. Shore ridge sands were poorly to very poorly sorted (mean = 1.95), outer lunette sands were moderately to poorly sorted (mean =

1.11), while sands from the linear dune and inner lunette were poorly sorted (mean = 1.47 and 1.69, respectively). Sample skewness ranged from fine to very fine skewed. Kurtosis at depth was very leptokurtic in all samples. However the surface samples of the linear dune and outer lunette were leptokurtic and mesokurtic, respectively.

Mean grain size generally decreased with depth at the four auger sites although there were localized increases at some sites. Linear dune sands decreased in mean grain size from 2.06 phi at the surface to 2.3 phi at the base. Mean sand size in the outer lunette decreased from 2.18 phi at the surface to 2.5 phi at 3m depth, then increased slightly before coarsening to 2.44 phi at the base (5m). Inner lunette sands decreased from 2.27 phi at the surface to 2.56 phi at 2 m before increasing to 2.52 phi at 3 m. Below 3 m mean grain size decreased to 2.55 phi at the base of the auger hole. The most marked decrease in grain size was in the shore ridge from 2.42 phi at the surface to 3.82 phi at 2.5 m depth, demonstrating that this dune is clearly distinct from the others.

Munsell colors for dry samples are shown in Fig.3.2 and Table 3.3. Color varied considerably between the four auger sites ranging from light yellow (almost white) to a dark reddish orange. Although similar in morphology, the two lunettes are very different in color. In fact, the outer lunette is similar in color to the red linear dune while the inner lunette is more like the yellow/white shore ridge. These color similarities/differences suggest that the inner lunette and shore ridge sands have undergone processes that the linear dune and outer lunette sands have not. This possibility will be explored later in the thesis.

Surface sediments in all four dunes were slightly darker than for deeper sediments, possibly because of more organic matter in the surface soil layer or due to bleaching of deeper sands by groundwater leaching iron. The surface color for the inner lunette was noticeably redder

than deeper sands, which might indicate mixing at the surface level between the inner yellow and outer red/orange lunette. However, even beyond the soil zone, both lunette dunes become lighter in color at greater depth, as does the linear dune and shore ridge. However, the outer lunette becomes generally lighter in color with depth although this trend is interrupted by slightly darker sediments at 2 m and 4.75 m. These horizons of slightly darker color could record a wetter climate coupled with a more stable dune in the past. This possibility is explored later in the thesis.

Chronology

OSL ages for the four auger sites are shown in Table 3.4 and Fig. 3.3. In all samples the distribution of aliquot ages was unimodal indicating a limited impact of bioturbation on the recorded ages. It should be noted, however, that the central OSL age for the inner lunette at 1m was slightly younger than the age of the 0.5 m sample, although both ages are statistically the same at the 2σ level. However, the 1.0 m OSL age was not included in calculations of sand accumulation rates because of "possible bioturbation" problems.

The youngest of the deposits examined was the shore ridge, which had an age of 2.18±0.17ka at 0.5m and a basal age at 2.5 m of 2.93±0.26 ka. The shore ridge represents the most recent period of ridge accumulation from ca. 3-2.0 ka and was clearly deposited quite rapidly during the late Holocene. The upper 4.1 m of the inner lunette and upper 5 m of the outer lunette were deposited within the last 75.67±8.87 ka and 74.17±8.56 ka, respectively, with the sand at 1 m dating to 9.21±1.09 ka and 14.91±1.64 ka. These generally similar age ranges for the two lunette dunes indicate that they were formed at roughly the same time and so should have experienced the same periods of stability and activity over the last 75 ka. The linear dune

provided an age of 35.12±4.04 ka at 3 m where calcrete nodules were encountered preventing further augering. At 3 m depth in the outer lunette the sand dated to 37.84±4.12 ka, but the sand at 3 m in the inner lunette was much older dating to 61.24±6.93 ka. However, sand at 2.0 m depth in the inner lunette provided an OSL age of 39.05±4.15 ka. These three ages suggest that the upper ca. 3 m of sands in all three dunes were deposited probably during the last ca. 40-45/50 ka .

Sediment accumulation rates were calculated based on the central OSL ages in order to identify periods of possibly increased/reduced deposition that might indicate differences in climatic conditions. The shore ridge accumulated most rapidly at a rate of approximately 200 cm/ka. The inner lunette accumulated at a fairly constant rate of 5.52cm/ka following a slightly more rapid period of deposition from 75.67±8.87 ka to 61.24±6.93 ka when it was accumulating at a rate of 7.62 cm/ka.

The outer lunette also appears to have accumulated more rapidly (7.87cm/ka) about the same time, from74.17±8.56 ka to 61.47±6.43 ka. The rate of deposition then slowed to 4.99cm/ka from 61.47±6.43 ka until 21.44±2.15 ka. From21.44±2.15 ka to 14.91±1.64 ka the dune grew much more rapidly at 15.31cm/ka until its growth slowed to 4.4cm/ka from 14.91±1.64 ka to 3.56±0.39 ka.

Based on the OSL age data, the linear dune accumulated at a more or less constant rate of 8.1 cm/ka from 35.12±4.04 ka to 4.29±0.44 ka. There does seem to be a very slight increase in the rate of accumulation to 9.34 cm/ka from 20.79±2.08 ka to 10.08±1.14 ka that correlates with a similar period of more rapid accumulation of the outer lunette during about the same period.

It should be noted, however, that the lunette auger sites were deliberately located away from the higher, central section of the lunette in the hope that the auger would pass through

sediments of greater age in the depth penetrated. However, this strategy may mean that vertical accumulation rates in the central part of the outer and inner lunettes could be higher than those reported here for the "horns" of the lunettes. However, changes in deposition with depth on the horns should parallel changes in the center of the lunette.

Magnetic Susceptibility

Average MS values for each dune site are shown in Table. 3.5. The shore ridge had the lowest average MS value of the four, 2.57E-08 m3/kg. Sands of the inner lunette and linear dune had much higher average MS values of 5.59E-08 m3/kg and 5.73E-08 m3/kg, respectively. Interestingly, the outer lunette sands had the highest average MS of 6.98E-08 m3/kg.

Variations in MS with depth are shown in Table 3.5 The linear and lunette dunes have increased MS at or near the surface possibly reflecting soil development. The shore ridge does not follow this pattern possibly because of the very young age of this deposit, giving little time for soil development to occur. MS of the linear dune decreases gradually with depth but superimposed on this overall trend are peaks in MS at 0.1, 1.0, and 2.2 m that could record increased soil development at these times. MS of inner lunette sands also decreases generally with depth although individual peaks occur at 0.3, 0.8 and 3.0 m depth. In contrast, MS values for outer lunette dune sands increase with depth with individual peaks at 0.1, 0.5, 1.9, 3.6, and 5.0 m. Finally, the shore ridge shows variable MS with peaks at 0.5 and 2.0 m with MS values lower than in the other dunes possibly because of the young (late Holocene) age of the ridge system.

Chemistry

Results of the 20 element ICPMS analyses are shown in Tables 3.6 & 3.7 and Fig. 3.4. This pretreatment was chosen to remove fairly soluble secondary precipitates. The data reveal marked differences between the inner lunette/shore ridge, and the outer lunette/linear dune. It would seem that the two red dunes are chemically more similar to each other than to either of the other two dunes. Silica (Si) is generally lower in the linear dune than in the outer lunette. Ca decreases with depth in both dunes although more quickly in the linear dune. Mg increases with depth in the outer lunette while remaining constant in the linear dune. Na increases with depth in both dunes but is more abundant in the outer lunette, probably because the outer lunette derives sediment from the pan, including precipitated salts, while the linear dune terminates at the upwind margin of the pan. Most intriguing is that the less mobile elements such as Al, Fe, Zn, and Mn decrease with depth in the linear dune and all but Al decrease with depth in the outer lunette dune.

The shore ridge and inner lunette, which are composed largely of yellow sand, have a few key chemical differences distinguishing them from each other and from the red dunes. For example, in the inner lunette Al is significantly higher than in any other dune samples. The less mobile elements Fe, Zn, and Mn are intermediate between values for samples from the red dunes and shore ridge, the latter containing very little Fe. Ca is significantly higher in both the inner lunette and the shore ridge, possibly because of close proximity to the pan shore floor and its location on the downwind side of the pan. The very mobile elements Na and Mg are higher in the shore ridge sediments and much lower in the other three dunes. This suggests that proximity to salt deposits on the floor of the pan and the young age of the sands is influencing chemical composition. K, Sr, and P are also higher in the shore ridge sands possibly also due to proximity

of salt crusts on the pan floor. There is a noticeable lack of Si (presumed to be microcrystalline silica) in the shore ridge sediments compared to the other dunes. This may suggest that these sediments have not been in place long enough for chemical weathering to have produced microcrystalline silica on the grains.

While there are some similarities between the shore ridge and the inner lunette dune, it is evident that the shore ridge is unique among the dunes studied here. The data indicate that the inner lunette dune lies chemically between the shore ridge and the two red dunes. Therefore, it is possible that its proximity to the shore ridge has allowed incorporation of windblown sediment from the shore ridge, resulting in an intermediate chemical character.

Chemical analysis of local well water samples (Table 3.8) revealed high amounts of Ca, K, Mg, Na, and Si. The greater abundance of K at Hugos2 and Toasis3, compared with Hugos7 is because Hugos7 is a protected well used by the local people, whereas the other two wells are used heavily by animals that wade in the water. Na is also higher in the two animal watering holes for the same reason. Si and Mg are relatively high in all three of the water samples examined, which is to be expected given the presence of silcretes and dolomitic limestones in the area. Ca was higher at Hugos7 presumably because of the local calcrete. The elements Na, K, Ca, and Sr were common in the shore ridge at Otjimaruru and in the waters sampled suggesting deposition of these salts in the pan floor during dry periods and incorporation in the shore ridge due to later aeolian activity.

SAMPLE	DEPTH (m)	MEAN (phi)	SORTING	SKEWNESS	KURTOSIS
Linear Dune (MURU-6)	0	2.06	1.29	0.36	1.45
	0.5	2.18	1.51	0.36	1.74
	1	2.27	1.39	0.25	1.65
	2	2.31	1.53	0.27	1.87
	3	2.35	1.47	0.21	1.69
	3.3	2.3	1.65	0.32	1.87
Average		**2.25**	**1.47**	**0.30**	**1.71**
Outer Lunette (MURU-19)	0	2.18	0.77	0.23	1.05
	0.5	2.4	1.12	0.29	1.64
	1	2.42	1.12	0.28	1.69
	2	2.48	1.18	0.28	1.88
	3	2.55	1.43	0.33	2.39
	4	2.49	0.94	0.16	1.46
	4.75	2.44	1.03	0.22	1.6
	5	2.44	1.28	0.3	2.13
Average		**2.43**	**1.11**	**0.26**	**1.73**
Inner Lunette (MURU-3)	0	2.27	1.41	0.29	1.84
	0.5	2.47	1.72	0.33	2.24
	2	2.56	1.75	0.37	2.07
	3	2.52	1.78	0.38	2.08
	4.1	2.55	1.79	0.39	2.04
Average		**2.47**	**1.69**	**0.35**	**2.05**
Shore Ridge (MURU-15)	0	2.42	1.84	0.31	1.99
	0.5	2.7	1.66	0.32	2.38
	1.1	2.69	1.64	0.31	2.47
	2	3.25	2.1	0.46	2.15
	2.5	3.82	2.52	0.55	1.91
Average		**2.98**	**1.95**	**0.39**	**2.18**

Table 3.1 Grain size statistics for dunes at Otjimaruru Pan.

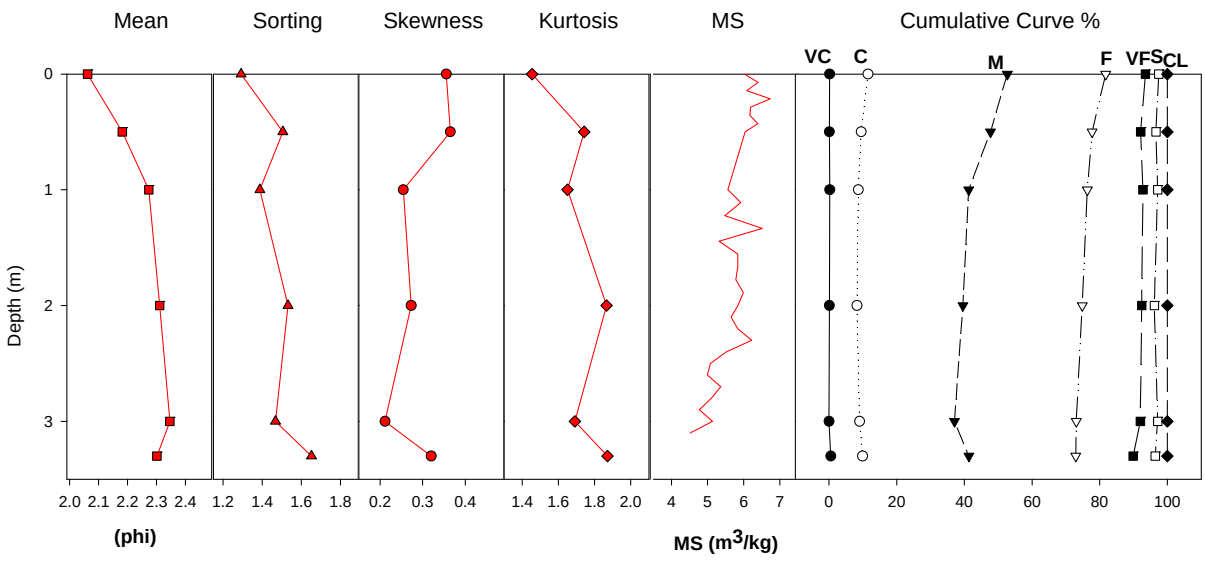

Fig. 3.1a Variations in grain size characteristics with depth in the Linear Dune (MURU-6)

Average	MEAN	SORTING	SKEWNESS	KURTOSIS
Linear Dune	2.25	1.47	0.30	1.71

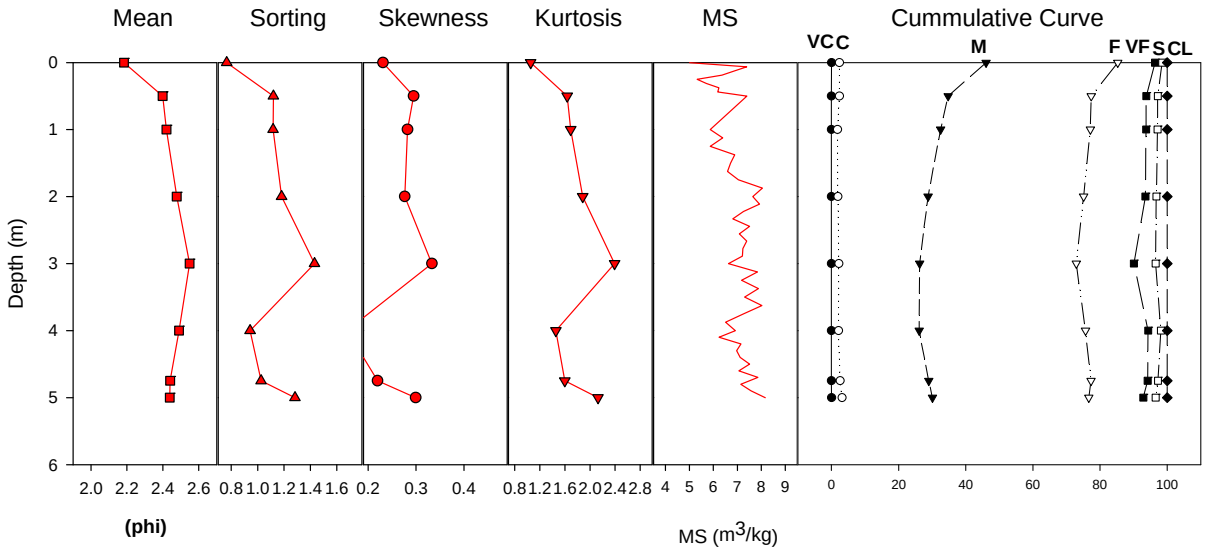

Fig. 3.1b Variations in grain size characteristics with depth in the Outer Lunette (MURU-19)

Average	MEAN	SORTING	SKEWNESS	KURTOSIS
Outer Lunette	2.42	1.11	0.26	1.73

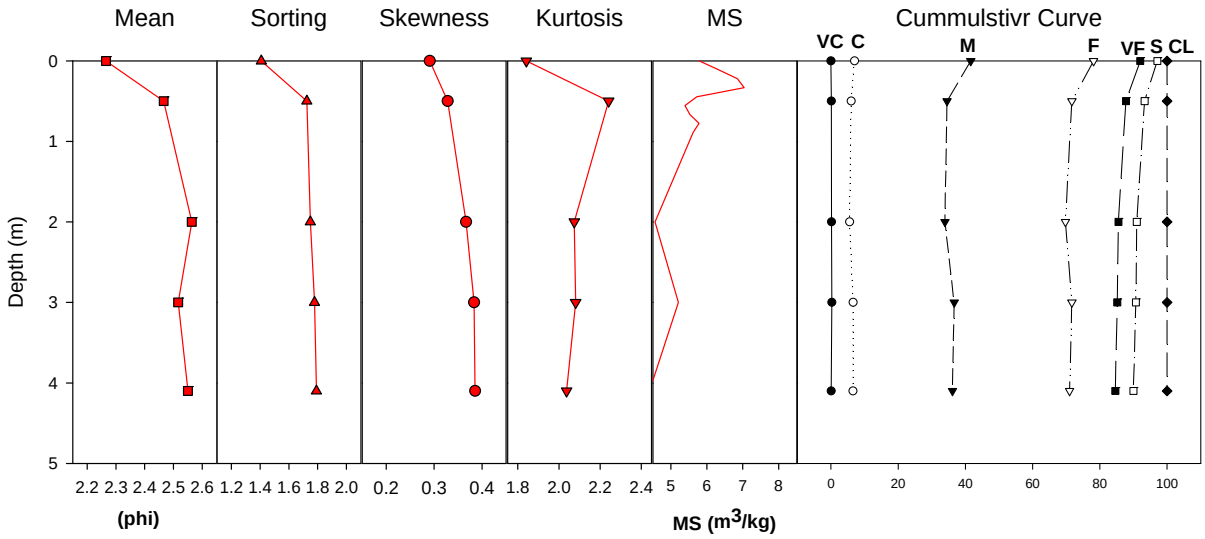

Fig. 3.1c Variations in grain size characteristics with depth in the Inner Lunette (MURU-3)

Average	MEAN	SORTING	SKEWNESS	KURTOSIS
Inner Lunette	2.47	1.69	0.35	2.06

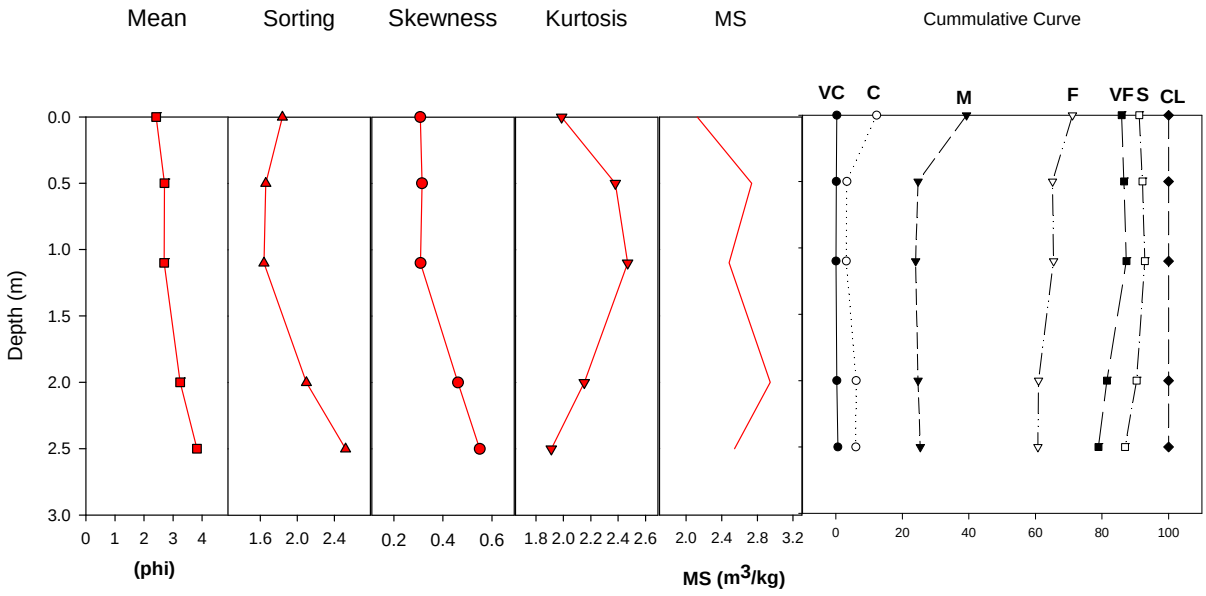

Fig. 3.1d Variations in grain size characteristics with depth in the Shore Ridge (MURU-15)

Average	MEAN	SORTING	SKEWNESS	KURTOSIS
Shore Ridge	2.98	1.95	0.39	2.18

Figures 3.1a,b,c,d various grain size statistics including Mean grain size, sorting, skewness, kurtosis, and MS at depth in m3/ka. The cumulative curve shows the percent of the sand fraction of the whole. The classes are: VC- very coarse, C-coarse, M-Medium, F-fine, VS-very fine, S-silt, and CL-clay.

		%						
	Depth (m)	Very Coarse Sand	Coarse Sand	Medium Sand	Fine Sand	Very fine Sand	Silt	Clay
Linear Dune (MURU-6)	0	0.13	11.37	41.20	29.10	11.73	3.94	2.53
	0.5	0.11	9.36	38.24	30.04	14.37	4.52	3.36
	1	0.19	8.48	32.63	35.08	16.44	4.34	2.84
	2	0.11	8.11	31.35	35.26	17.63	3.71	3.83
	3	0.00	9.04	28.02	36.01	18.94	5.15	2.84
	3.3	0.53	9.39	31.41	31.58	16.96	6.54	3.59
Average		**0.18**	**9.29**	**33.81**	**32.85**	**16.01**	**4.70**	**3.16**
Outer Lunette (MURU-19)	0	0.05	2.30	43.69	39.24	11.11	2.15	1.47
	0.5	0.00	2.37	32.38	42.63	16.41	3.40	2.81
	1	0.00	1.79	30.74	44.61	16.62	3.38	2.86
	2	0.00	1.93	26.86	46.30	18.41	3.29	3.20
	3	0.00	2.22	24.06	46.65	17.16	6.52	3.39
	4	0.00	2.09	24.04	49.54	18.68	3.82	1.83
	4.75	0.00	2.58	26.39	48.37	16.87	3.04	2.75
	5	0.03	3.10	26.95	46.62	16.20	3.70	3.41
Average		**0.01**	**2.30**	**29.39**	**45.49**	**16.43**	**3.66**	**2.72**
Inner Lunette (MURU-3)	0	0.00	7.00	34.58	36.54	13.92	5.09	2.87
	0.5	0.08	5.94	28.50	37.19	16.09	5.54	6.67
	2	0.15	5.38	28.38	35.86	15.75	5.49	8.99
	3	0.26	6.30	30.10	34.99	13.53	5.55	9.26
	4.1	0.05	6.48	29.61	34.85	13.61	5.40	9.99
Average		**0.11**	**6.22**	**30.23**	**35.89**	**14.58**	**5.41**	**7.56**
Shore Ridge (MURU-15)	0	0.30	12.00	27.00	31.81	14.79	5.29	8.82
	0.5	0.16	3.16	21.41	40.42	21.45	5.57	7.82
	1.1	0.05	3.09	20.87	41.43	21.92	5.54	7.11
	2	0.32	5.77	18.63	36.25	20.52	8.93	9.58
	2.5	0.59	5.40	19.39	35.35	18.20	7.99	13.08
Average		**0.28**	**5.88**	**21.46**	**37.05**	**19.37**	**6.67**	**9.28**

Table 3.2 percent values for seven grain size classes in samples from the four augered dunes.

	Average %						
Sample	**Very Coarse Sand**	**Coarse Sand**	**Medium Sand**	**Fine Sand**	**Very fine Sand**	**Silt**	**Clay**
Linear Dune	0.18	9.29	33.81	32.85	16.01	4.70	3.16
Outer Lunette	0.01	2.30	29.39	45.49	16.43	3.66	2.72
Inner Lunette	0.11	6.22	30.23	35.89	14.58	5.41	7.56
Shore Ridge	0.28	5.88	21.46	37.05	19.37	6.67	9.28

Sample Site	Depth (m)	Munsell Color
MURU-6	0	5YR 5/6
	0.5	5YR 5/8
	1	5YR 5/8
	2	5YR 5/8
	3	5YR 5/8
	3.3	5YR 5/8
MURU-19	0	5YR 6/6
	0.5	5YR 5/6
	1	5YR 5/8
	2	5YR 5/8
	3	5YR 5/8
	4	5YR 5/8
	4.75	5YR 5/8
	5	5YR 6/8
MURU-15	0	2.5Y 7/1
	0.5	10YR 7/3
	1	10YR 7/3
	2	10YR 7/4
	2.5	10YR 7/3
MURU-3	0	10YR 6/4
	0.5	10YR 6/4
	2	10YR 8/3
	3	10YR 8/2
	4.1	10YR 8/2

Table 3.3 Dry Munsell Color of samples from different depths in the four dunes.

Fig. 3.2 Color variations by depth in samples from the four dunes.

Sample	Depth (m)	Grain size (µm)	Aliquots	De (Gy)	U (ppm)	Th (ppm)	K (%)	Water content (%)	Cosmic dose rate (Gy/ka)	Dose rate (Gy/ka)	Age (ka) (Error: 2 σ)
Inner Lunette											
MURU-3	**0.5**	125-180	16	13.19±0.60	0.89±0.14	3.26±0.51	0.60±0.1	5±2.5	0.25	1.26±0.11	10.49±1.06
	1	125-180	18	10.91±0.71	0.82±0.16	2.88±0.57	0.58±0.1	5±2.5	0.24	1.19±0.12	9.21±1.09
	2	125-180	16	46.61±1.20	1.59±0.19	1.75±0.69	0.53±0.1	5±2.5	0.2	1.19±0.12	39.05±4.15
	3	125-180	16	66.91±2.26	1.11±0.17	2.16±0.61	0.53±0.1	5±2.5	0.18	1.09±0.12	61.24±6.93
	4.1	125-180	19	77.50±1.17	1.18±0.18	1.92±0.64	0.48±0.1	5±2.5	0.16	1.02±0.12	75.67±8.87
Linear Dune											
MURU-6	**0.5**	125-180	16	5.76±0.20	1.34±0.21	4.17±0.77	0.51±0.1	5±2.5	0.25	1.34±0.13	4.29±0.44
	1	125-180	18	12.63±0.62	1.2±0.21	2.73±0.75	0.57±0.1	5±2.5	0.24	1.25±0.13	10.08±1.14
	2	125-180	19	24.25±0.50	1.16±0.14	2.48±0.5	0.55±0.1	5±2.5	0.2	1.17±0.11	20.79±2.08
	3	125-180	19	40.53±1.92	1.37±0.18	1.79±0.65	0.56±0.1	5±2.5	0.18	1.15±0.12	35.12±4.04
Shore Ridge											
MURU-15	**0.5**	125-180	19	3.97±0.06	2.35±0.25	2.59±0.86	0.89±0.1	5±2.5	0.25	1.82±0.14	2.18±0.17
	2	125-180	17	4.89±0.14	2.05±0.24	2.14±0.83	0.89±0.1	5±2.5	0.2	1.67±0.14	2.93±0.26
Outer Lunette											
MURU19	**0.5**	125-180	10	4.24±0.24	0.89±0.13	2.84±0.49	0.56±0.1	5±2.5	0.25	1.19±0.11	3.56±0.39
	1	125-180	15	15.75±0.51	0.71±0.13	2.11±0.48	0.53±0.1	5±2.5	0.24	1.06±0.11	14.91±1.64
	2	125-180	17	26.39±0.69	0.95±0.14	2.35±0.68	0.68±0.1	5±2.5	0.2	1.23±0.12	21.44±2.15
	3	125-180	19	41.98±0.98	0.78±0.17	2.53±0.62	0.60±0.1	5±2.5	0.18	1.10±0.12	37.84±4.12
	4	125-180	17	63.93±1.21	0.87±0.1	1.18±0.36	0.63±0.1	5±2.5	0.16	1.04±0.11	61.47±6.43
	5	125-180	16	71.71±1.38	0.73±0.12	1.54±0.46	0.58±0.1	5±2.5	0.14	0.97±0.11	74.17±8.56

Table 3.4 OSL age data for samples from dunes at Otjimaruru Pan, Namibia. (Error terms in 2 standard deviations).

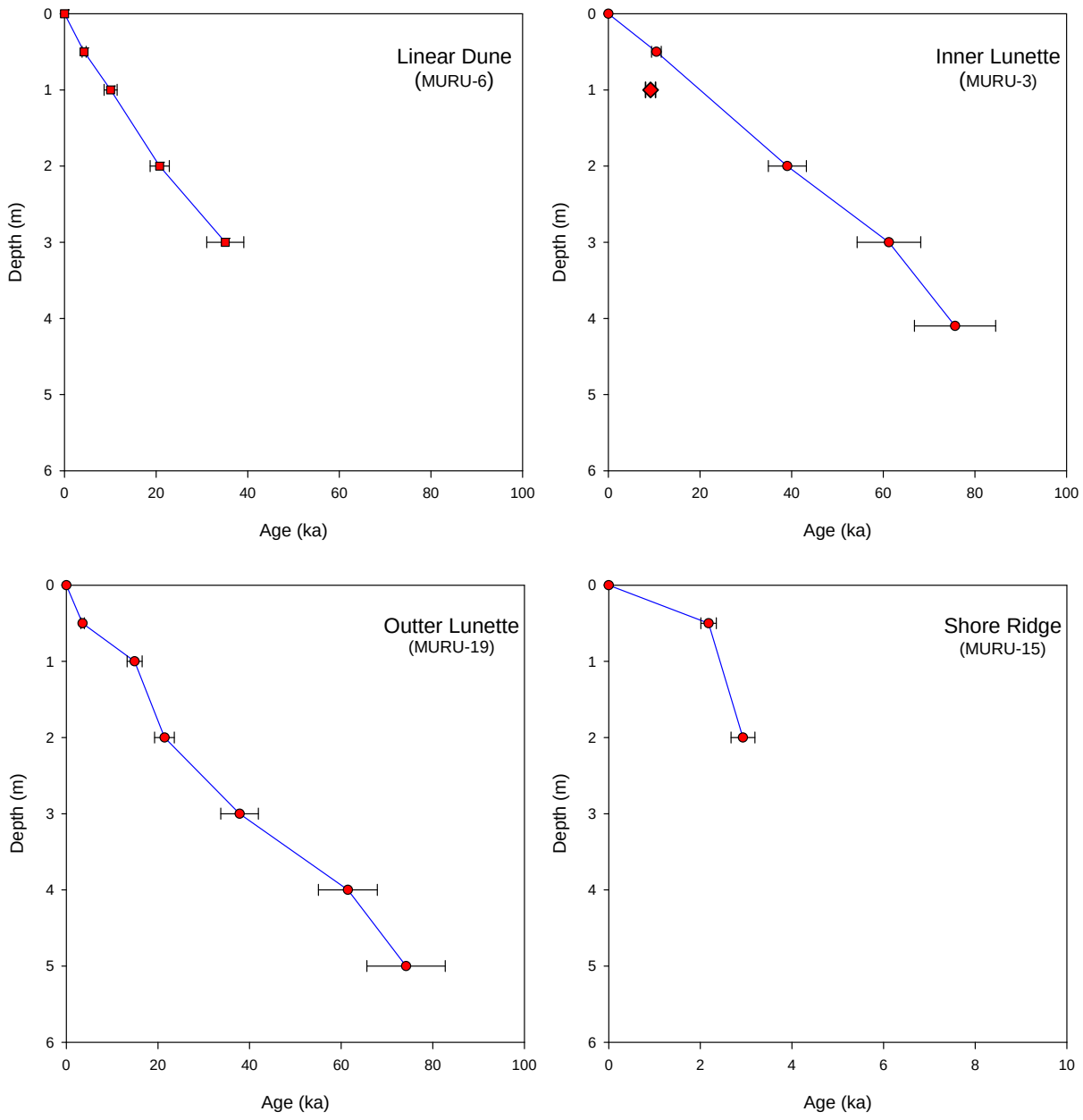

Fig. 3.3a Depth-age relationships in the Otjimaruru dunes. OSL ages and uncertainties are shown.

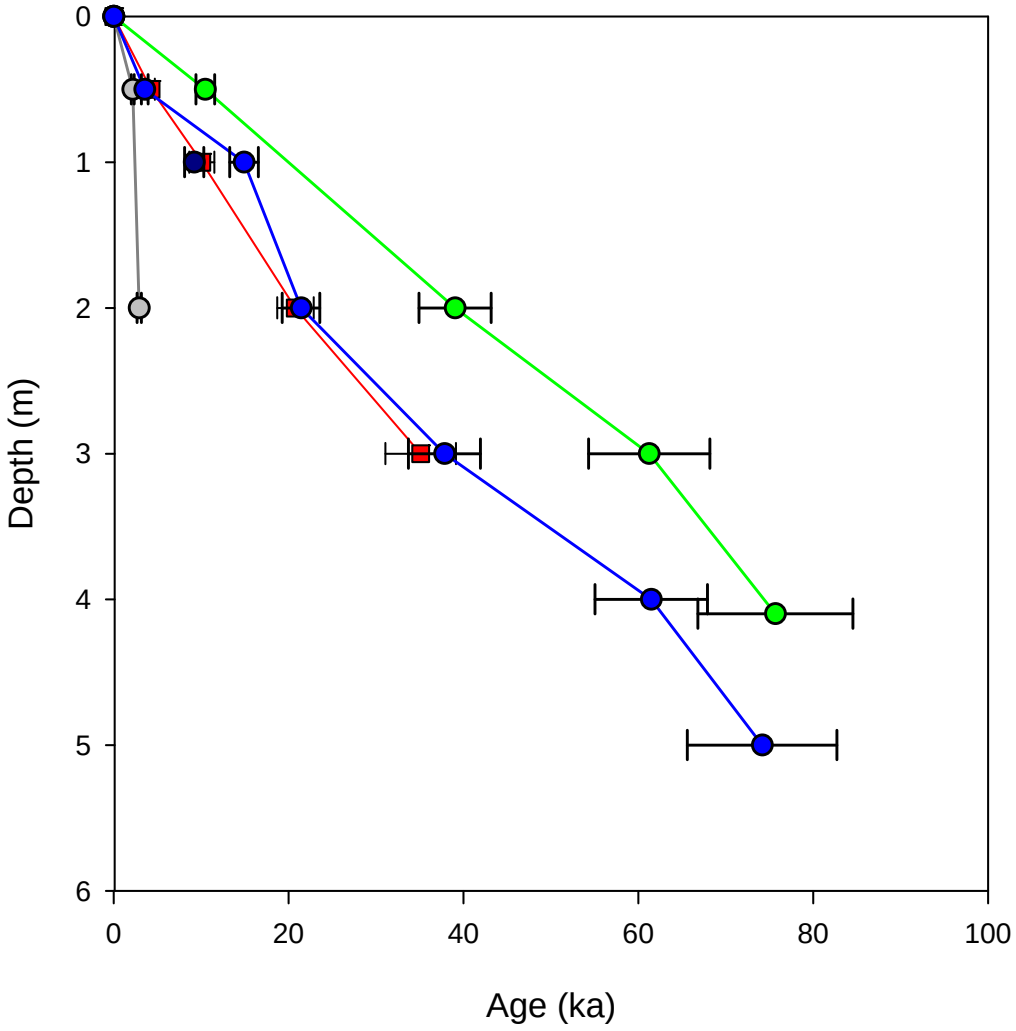

Fig. 3.3b Age-depth comparison for the shore ridge (grey), linear dune (red), outer lunette (blue), and inner lunette (green) at Otjimaruru Pan. OSL ages and errors are indicated.

Site	Depth (m)	MS Value	Error
Inner (MURU-3)	0	5.79E-08	3.32E-10
	0.111	6.34E-08	4.45E-10
	0.222	6.85E-08	6.39E-10
	0.333	7.04E-08	1.77E-10
	0.444	5.72E-08	1.84E-10
	0.555	5.40E-08	6.18E-10
	0.666	5.53E-08	4.71E-10
	0.777	5.78E-08	4.96E-10
	0.888	5.62E-08	1.78E-10
	2	4.56E-08	1.99E-10
	3	5.21E-08	4.67E-10
	4.1	4.40E-08	3.07E-10
Average		**5.69E-08**	**3.76E-10**

Site	Depth (m)	MS Value	Error
Shore (MURU-15)	0	2.13E-08	1.69E-10
	0.5	2.74E-08	3.45E-10
	1.1	2.48E-08	6.48E-10
	2	2.95E-08	3.88E-10
	2.5	2.54E-08	5.56E-10
Average		**2.57E-08**	**4.21E-10**

Site	Depth (m)	MS Value	Error
Linear (MURU-6)	0	6.02E-08	4.43E-10
	0.0714	6.40E-08	3.66E-10
	0.1428	6.08E-08	5.57E-10
	0.2142	6.73E-08	1.61E-10
	0.2856	6.19E-08	3.14E-10
	0.357	6.17E-08	6.29E-10
	0.4284	6.39E-08	4.15E-10
	0.5	6.04E-08	1.97E-10
	1	5.56E-08	5.40E-10
	1.111	5.92E-08	9.29E-10
	1.222	5.47E-08	4.92E-10
	1.333	6.51E-08	5.55E-10
	1.444	5.32E-08	4.36E-10
	1.555	5.84E-08	4.16E-10
	1.666	5.84E-08	3.15E-10
	1.777	5.78E-08	6.92E-10
	1.888	5.99E-08	4.74E-10
	2	5.84E-08	5.85E-10
	2.1	5.65E-08	1.88E-10
	2.2	5.83E-08	7.08E-10
	2.3	6.22E-08	3.37E-10
	2.4	5.52E-08	4.88E-10
	2.5	5.08E-08	6.35E-10
	2.6	5.00E-08	5.36E-10
	2.7	5.36E-08	4.71E-10
	2.8	5.10E-08	1.78E-10
	2.9	4.77E-08	5.59E-10
	3	5.14E-08	6.56E-10
	3.1	4.52E-08	1.59E-10
Average		**5.73E-08**	**4.63E-10**

Site	Depth	MS	Error
Outer Lunette (MURU-19)	0	5.01E-08	6.11E-10
	0.0625	7.40E-08	4.91E-10
	0.125	6.87E-08	4.90E-10
	0.1875	6.36E-08	4.56E-10
	0.25	5.32E-08	6.97E-10
	0.3125	5.71E-08	3.30E-10
	0.375	6.23E-08	4.27E-10
	0.4375	6.18E-08	5.57E-10
	0.5	7.40E-08	6.05E-10
	1	5.87E-08	3.81E-10
	1.125	6.39E-08	1.94E-10
	1.25	5.87E-08	6.54E-10
	1.375	6.89E-08	2.96E-10
	1.5	6.72E-08	2.94E-10
	1.625	6.58E-08	5.41E-10
	1.75	7.04E-08	4.00E-10
	1.875	8.05E-08	1.96E-10
	2	7.65E-08	4.34E-10
	2.111	7.92E-08	4.75E-10
	2.222	7.25E-08	5.13E-10
	2.333	6.81E-08	1.71E-10
	2.444	7.51E-08	3.90E-10
	2.555	7.08E-08	8.88E-16
	2.666	7.39E-08	5.02E-10
	2.777	7.24E-08	5.53E-10
	2.888	7.21E-08	3.16E-10
	3	6.63E-08	4.50E-10
	3.125	7.84E-08	2.92E-10
	3.25	7.17E-08	6.39E-10
	3.375	7.88E-08	3.11E-10
	3.5	7.31E-08	5.31E-10
	3.625	8.02E-08	6.62E-10
	3.75	7.26E-08	5.98E-10
	3.875	6.51E-08	6.88E-10
	4	6.91E-08	7.04E-10
	4.1	6.24E-08	3.25E-10
	4.2	7.16E-08	1.58E-10

Outer Lunette (MURU-19) cont.	4.3	6.97E-08	4.81E-10
	4.4	7.12E-08	4.35E-10
	4.5	7.51E-08	5.88E-10
	4.6	7.07E-08	6.06E-10
	4.7	7.86E-08	1.69E-10
	4.8	7.15E-08	4.15E-10
	4.9	7.57E-08	0
	5	8.17E-08	1.68E-10
Average		**6.98E-08**	**4.27E-10**

Table 3.5. MS data for the Otjimaruru dunes by depth.

Element	Linear Dune 0.14m	Linear Dune 3.1m	Outer Lunette 0.12m	Outer Lunette 2m	Outer Lunette 4.1m	Inner Lunette 0.3m	Shore Ridge 1.1m
Al	47.12	26.5	56	48	51.58	94.79	4.487
B	0.103	0.093	0.1	0.1	0.0831	0.2426	0.6213
Ba	1.622	1.223	1.28	1.4	0.8761	1.171	3.135
Ca	289.3	86.33	301	194	220.4	4995	5943
Cd	0.053	0.0658	0.07	0.1	0.1448	0.1053	0.1251
Co	0.093	0.1345	0.1	0.1	0.1378	0.1313	0.0554
Cr	0.051	0.0181	0.02	0	0.0317	0.256	0.3003
Cu	0.222	0.1409	0.22	0.1	0.0959	0.5367	0.0555
Fe	13.37	9.507	15.6	12	11.22	8.331	0.449
K	37.9	27.68	44.6	40	21.62	45.5	91.59
Mg	40.92	42.16	50.6	79	80.43	77.24	122.8
Mn	5.565	1.536	6.01	2.8	1.828	7.293	1.674
Mo	0.158	0.0746	0.13	0.1	0.1036	0.1202	0.0953
Na	8.496	13.82	11.7	8.8	59.45	11.87	486.2
Ni	0.132	0.0472	0.12	0.1	0.0712	0.3369	0.1016
P	2.251	1.304	6.33	2.3	2.238	23.43	53.66
Pb	0.256	0.1928	0.3	0.2	0.2034	0.9344	0.8082
Si	28.45	28.36	35.4	50	54.08	46.1	10.91
Sr	1.06	0.7565	3.8	2.5	2.351	33.24	85.42
Zn	10.37	2.788	12	4	3.583	5.001	0.1594

Table 3.6. Chemical abundance (ppm) of 20 elements in selected samples from the Otjimaruru dunes.

Sample Site	Depth	Less Mobile Elements				More Mobile Elements						
		Al	Fe	Zn	Mn	Si	Ca	Mg	Na	K	Sr	P
Linear Dune	(m)	**47.12**	**13.37**	**10.37**	**5.565**	28.45	**289.3**	40.92	**8.496**	37.9	1.06	2.251
	3.1	**26.5**	**9.507**	**2.788**	**1.536**	28.36	**86.33**	42.16	**13.82**	27.68	0.7565	1.304
Outer Lunette	**0.12**	55.96	**15.57**	**12.04**	**6.006**	**35.43**	**301**	**50.57**	**11.67**	**44.55**	3.804	6.33
	2	48.15	**12.03**	**3.956**	**2.844**	**50.26**	**194.1**	**79.1**	**8.807**	**40.39**	2.54	2.276
	4.1	51.58	**11.22**	**3.583**	**1.828**	**54.08**	**220.4**	**80.43**	**59.45**	**21.62**	2.351	2.238
Inner Lunette	**0.3**	94.79	8.331	5.001	7.293	46.1	4995	77.24	11.87	45.5	33.24	23.43
Shore Ridge	**1.1**	4.487	0.449	0.1594	1.674	10.91	5943	122.8	486.2	91.59	85.42	53.66

Increase with depth

Decrease with depth

Table 3.7. Chemical data from selected dune samples showing variations between dunes and with depth.

Element	*Hugus2*	*Hugus7*	*Toasis3*
Al	0.22	0.28	0.26
B	0.43	0.18	0.51
Ba	0.09	0.20	0.14
Ca	32.48	100.40	35.91
Cd	0.02	0.03	0.04
Co	0.02	0.02	0.03
Cr	0.05	0.06	0.06
Cu	0.03	0.04	0.05
Fe	0.02	0.00	0.02
K	60.52	9.96	96.85
Mg	22.45	29.04	36.70
Mn	0.01	0.01	0.02
Mo	0.03	0.03	0.03
Na	255.60	104.40	275.50
Ni	0.04	0.04	0.04
P	0.56	0.56	1.21
Pb	0.14	0.19	0.21
Si	18.45	40.17	32.34
Sr	0.65	0.71	0.78
Zn	0.02	0.01	0.01

Table 3.8 Chemical elements (ppm) in groundwater from pans near Otjimaruru.

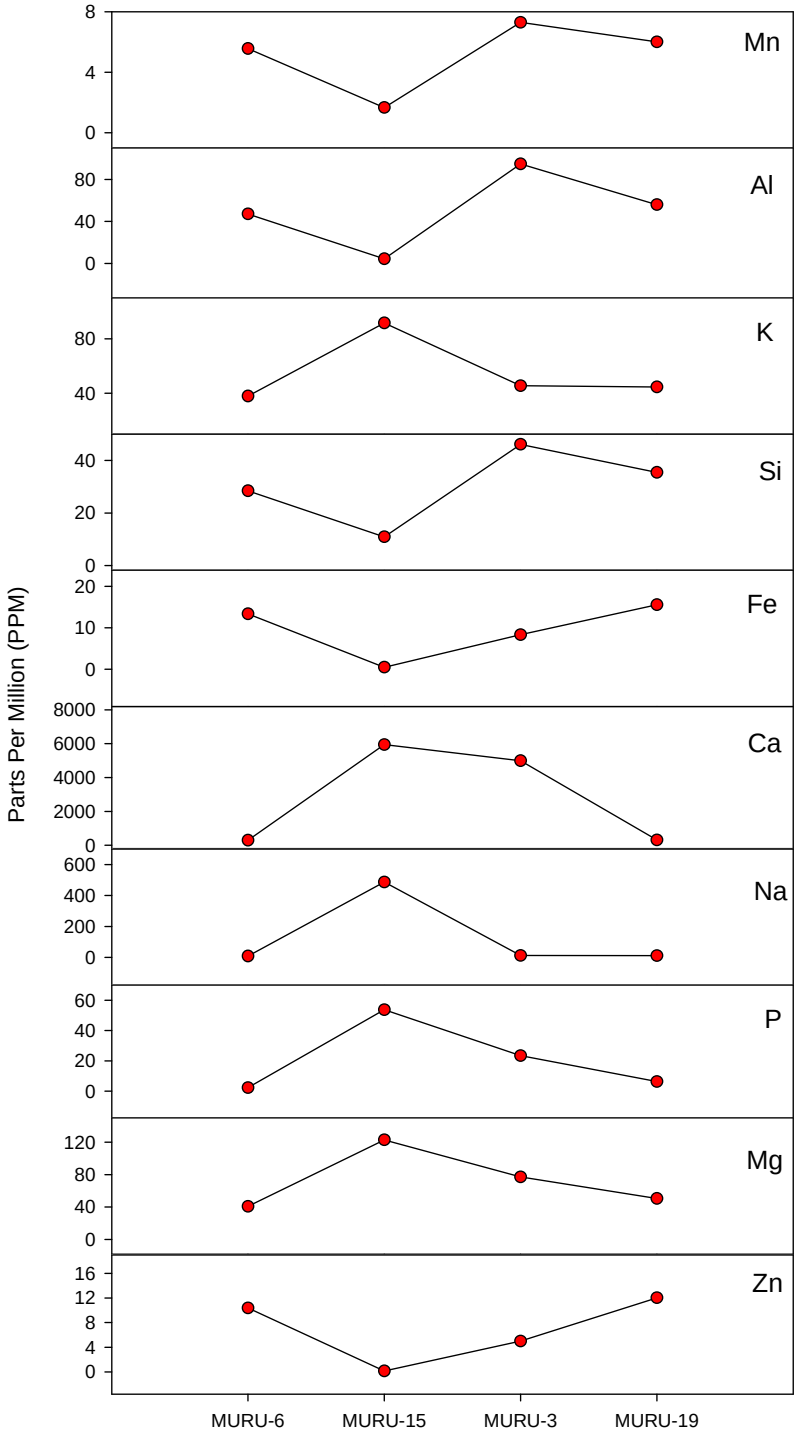

Fig. 3.4 Variations in chemistry between the four dunes from north to south in the downwind direction (MURU-6 = linear dune; MURU-15 = shore ridge; MURU-3 = inner lunette; MURU-19 = outer lunette.

CHAPTER 4

THE ORIGIN AND PALEOENVIRONMENTAL HISTORY OF THE OTJIMARURU PAN-LUNETTE SYSTEM

Origin of the Pan and Surrounding Dunes

Several hypotheses have been proposed for the formation of pans and their associated lunette dunes. The first and most widely accepted is the deflation model in which the pan and lunette dune are created during dry periods of climate by deflation (Grove 1969, Lancaster 1978, Goudie and Wells 1995). The second hypothesis is one that sees wave action, associated with wetter, windier periods, deposit sediment along the shoreline, which is then reworked into a lunette dune on the downwind side of the pan (Bowler 1986, Bowler 1973). A third hypothesis for the origin of the pans is that they form along ancient drainage lines (Grove 1969). The final and oldest theory for the origin of the pans involves animal trampling in low-lying areas where water has pooled (Goudie 1989, Grove 1969). This process leads to the gradual removal of soil, caked to the hides of the animals when they leave the muddy area. Over time, the loss of soil increases the size of the depression ultimately forming a pan The animal trampling and drainage line hypotheses have largely been abandoned in favor of the deflation and wave action hypotheses but the effects of animals on the pans cannot be entirely discounted. At Otjimaruru the pan floor was littered with animal tracks but the very large number of pans compared to the past number of animals makes this hypothesis unlikely for the primary origin of pans. Also arguing against an animal origin is that pans are much more common in the drier southern

Kalahari where animal populations would likely be at their lowest. In addition, there is no doubt that some pans have formed along drainage lines but it is difficult to see how this mode of formation can explain the huge numbers of pans that occur.

Based on the data obtained from Otjimaruru it is clear that the deflation model alone cannot explain the formation of this pan-lunette system. The prevailing wind characteristics of the region produce linear dunes, and to create a basin for deflation there must be a mechanism to remove the linear dunes. In addition, the area is underlain by calcrete and silcrete that negate, or at least limit the likelihood of deflation. In addition, the deflation hypothesis does not explain why linear dunes almost never cross or cover pan floors. Under dry conditions linear dune systems should dominate the landscape and cover the pan floors over time.

The second hypothesis for the formation for pans and lunettes fits more easily with data collected at Otjimaruru. The data indicate that the initial formation of pans may be associated with springs along faults where groundwater can more easily come to the surface. Regardless, pans seem to form in areas where there is a high groundwater table. When groundwater levels are high enough for the water to reach the surface, during wetter periods, the surface water interacts with pre-existing linear dunes, disrupting and distorting them around the future pan. Satellite imagery shows linear dunes in the initial and later stages of modification by pan water bodies to form lunettes (Fig.4.1.). The satellite images also show that linear dunes end at the upwind margins of pans, indicating that periodic flooding of the pan prevents their extension across the pan.

Water in the pan does two things. The high groundwater table modifies the linear dunes by wave erosion and sediment is transported via longshore drift in the downwind direction to begin the formation of a shore ridge and ultimately a lunette dune. The presence of water also

deepens the pan through chemical weathering and leaching of soluble elements. High levels of dissolved solids may ultimately lead to the formation of chemical precipitates on the floor of the pan that are later eroded by wind along with some clays, effectively deepening the pan. This increases the frequency of flooding in the pan as the floor of the pan is now at a lower elevation relative to the ground water table. For pan development, flooding must be frequent enough so that re-generation of the linear dunes in the pan surface is not possible.

Based on chemical analysis of groundwater samples taken from nearby pans, the local groundwater chemistry can be characterized as having a fairly high amount of dissolved Ca, Mg, Na, and Si. These dissolved solids are also found in higher concentrations in dunes that are believed to have been submerged by water in the pan at some point. The chemical composition of the ground water and the local bedrock may determine the nature of the chemical precipitate that results from evaporation of the water in the pan. High calcium carbonate concentrations will lead to calcrete deposition around the margins of the pan and also across its floor. Under more arid conditions, silica may precipitate because of alkaline conditions of the drying pan, forming silcretes and this has occurred at Otjimaruru across the pan floor. Over time, as the pan deepens it becomes smaller. This is because a small deep pan can hold the same amount of water as a larger shallow pan. When this happens the calcrete deposits are left "high and dry" and frequently form a low cliff around the smaller pan. This has occurred both at Otjimaruru and at nearby Aminuis Pan. If the material precipitated on the floor of the pan is silcrete, as in the case of Otjimaruru, it is difficult to see how aeolian deflation can play much of a role in deepening the pan once the crust is formed.

The fact that the process begins with the linear dune system already in place indicates an ancient period of dry conditions along with massive dune development. The oldest ages at

Otjimaruru were 78ka and at nearby Aminuis ages were twice that at 160ka (Brook, personal communication, April 2011).

The inner and outer lunette dunes, although different in color, appear to have been formed at approximately the same time. The marked difference in color could indicate that the red outer lunette is older than the yellow inner lunette because it has had more time to acquire the red color (red dunes are frequently regarded as older than lighter-colored dunes). However, the OSL ages show that this is not the case. At 6 m depth both the inner and outer lunette dunes have about the same age, the inner lunette dating to 78.1ka and the outer lunette to 74.8ka. However, both dunes extend much deeper than 6 m and the floor of the pan is considerably deeper than the depth of the core could penetrate indicating that the lunettes are much older than these ages. The implications are that these two dunes formed at the same time despite being different distances from the pan itself. The deflation model of pan development does not explain this well. However, in the flooding model, the erosion and reworking of the linear dunes by the lake water, with the formation of a red outer lunette dune, would be accompanied by the formation of a second contemporaneous inner lunette dune as winds and waves transported yellow sand downwind across the pan. Once these dunes were in place they disrupted the well-defined bimodal wind flow that formed the linear dune field thereby retarding the development of linear dunes immediately downwind of the pan.

This model not only explains the presence of two lunette dunes but may also hint at the reason behind the color difference. On the upwind margin of the pan are red linear dunes that do not cross into the pan because of the seasonal water body that occupies it. If sand is blown into the pan while there is water present, the sand will be washed by waves and abrasion will dislodge iron from the grain surfaces (Levin et al. 2007). Immediately downwind of the pan is a low shore

ridge that is a light yellow brown in color followed by the inner lunette, which has a similar light color. In contrast, the outer lunette dune is red and most similar to linear dunes in the area. The implication is that the shore ridge and inner lunette have a similar origin in that the dune sand was at one time washed by water in the pan and "cleaned" of iron oxide. In contrast, the sands of the outer lunette and surrounding linear dunes never crossed the pan and so retained their distinctive red color.

The chemistry of the outer lunette and the linear dune supports the above conclusion. The linear dune and outer lunette have similar percentages of Fe and Zn while the shore ridge has almost no Fe or Zn. Interestingly; the inner lunette has intermediate levels of Fe and Zn. This may suggest that the shore ridge sands are ultimately incorporated into the inner lunette, effectively diluting the contents of Fe and Zn. The opposite appears to be the case with Sr, P, and Mg. These are in low abundance in the linear and outer lunette dunes, much more abundant in the shore ridge and at intermediate levels in the inner lunette. The highly mobile elements K and Na are present in much higher percentages in the shore ridge than in the other dunes. This may be because the shore ridge is very young (ca. 3-2 ka) and there has not been enough time for these elements to be leached from the sands by rain. The presence of higher K and Na in the shore ridge, elements that are also common in the ground waters of the area, indicates that the shore ridge was formed when there was water in the pan. Overall, the chemical data support the idea that there was a more permanent body of water in the pan in the past and that while similar in morphology the inner and outer lunettes share a different origin. The outer lunette is chemically very similar to the surrounding linear dunes suggesting that its sands never passed through the pan when it contained water. In contrast, the inner lunette is very different to the

surrounding linear dunes and to the outer lunette dune, in terms of color and chemistry, suggesting a completely different origin.

Stages in the Formation of Pan-lunette Systems

Data from Otjimaruru and satellite images of other dunes in the southern Kalahari have allowed identification of three basic stages in the development of pan lunette systems in the Kalahari. These stages are illustrated in Figs 4.1 and 4.2. The stages are:

Stage 1

Stage 1 is a long period of linear dune development that produces extensive fields of linear dunes over broad areas (stage 1 in Fig. 4.1 and 4.2). There are no pans but it is likely that rare, flash floods cause occasional ponding of water in localized interdune areas.

Stage 2

During Stage 2 a wetter climate causes groundwater levels to rise promoting localized spring activity, particularly along faults. This flow of groundwater to the surface produces a series of shallow lakes in low-lying interdune areas. In some cases the lakes may be large enough to inundate the bases of some linear dunes. If the lakes are long lasting, wave action at the lake shore erodes the slopes of inundated linear dunes, particularly on the downwind margin of the lake with the formation of a beach ridge or rudimentary lunette dune. The linear dunes on the downwind margin of the pan are modified by both the water in the pan and the effect the pan has on the local wind. As a result, these linear dunes are "blunted", becoming wider at their upwind ends (Figs 4.1a and 4.1b). Another change during

Stage 2 is that linear dunes running parallel to the pan (east and west of the pans in Fig. 4.1) begin to curve slightly around the pan at its downwind margin connecting to some degree with the blunted linear dunes there, adding to the developing "outer lunette dune".

Stage 3

Stage 3 sees the coalescence of the blunted ends of the linear dunes on the downwind margin of the pan, as well as a linking of the curved linear dunes on either side, resulting in the development of a complete lunette dune. A lighter colored inner lunette dune also forms during Stage 3 more or less concurrently with the final formation of the outer red lunette dune. Most researchers have until now regarded a double lunette as evidence of two separate dune building events. However, in the model presented hear the inner lunette develops around the same time as the outer lunette, which explains why OSL ages for the two lunette dunes at Otjimaruru are similar. The inner and outer lunettes differ in color and chemistry because the sand of the inner lunette was reworked by waters in the pan before being added to the lunette systems at the downwind margin of the pan. Wave action and/or anaerobic microbial activity removed iron from the sand making it very different from sand in the outer lunette, which still preserved its coating of iron.

Once the pan-lunette system has formed it will be preserved as long as the pan floods frequently enough to prevent the reestablishment of linear dunes across the pan and the erosion of the lunette system on the downwind margin. However, if the climate becomes significantly drier and the wind stronger, and this situation is maintained for a considerable time, the linear dunes in the area will become active and return the pan to its original form as merely part of a field of linear dunes with interdune areas that rarely contain standing water. This said, it seems

likely that once a pan/lunette system has formed, and the pan is gradually deepened by chemical weathering of its floor and removal of the weathered products by wind, the pan would be likely to survive. This is because the floor of the pan would be nearer to the local/regional ground water table and so more likely to flood at regular intervals.

Complicating this model for pan/lunette development is the role of calcrete, which is very common in areas with pans. The exact age of the calcrete is not known for certain; some calcrete may be of Kalahari System age while other calcrete may be Quaternary. If the calcrete is very old it would have been present at the time the major linear dune field in the southern Kalahari developed. The calcrete would have underlain the interdune areas causing surface ponding of water after rare rains. In this environment pans would have formed initially over calcrete substrate and would have increased in size and depth as the underlying calcrete was dissolved by the lake waters of the pan. This might explain the widespread occurrence of calcrete scarps around the margins of many pans.

Another possibility is that calcrete development accompanied the formation and evolution of pans as shown in Fig. 4.2. In this case, calcrete is formed at the level of the water table near the margin of the pan in the surrounding sands. Over time, as the pan is deepened by a combination of chemical

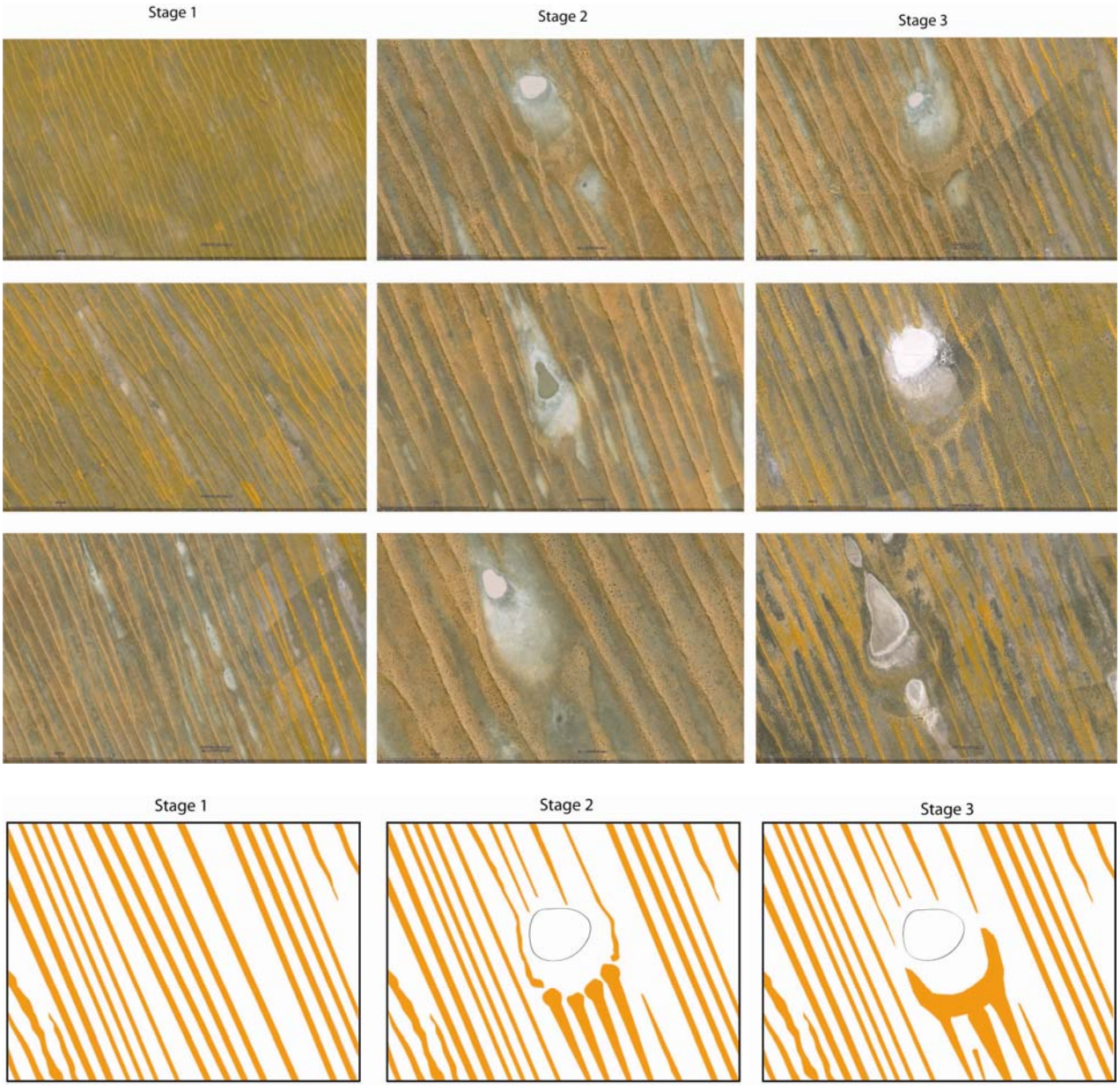

Fig. 4.1 Google Earth satellite images (a) and line drawings (b) depicting the three main stages of pan/lunette development in the southern Kalahari Desert. Stage1: undisturbed linear dune system. Stage2: formation of a pan and disruption of the linear dunes by water and blunting of linear dunes on the downwind margin of the pan. Stage 3: coalescence of the blunted upwind ends of the linear dunes forming a lunette dune.weathering and deflation so that the water level in the pan during the wet season drops gradually. This occurs despite the pan retaining the same volume of water because a smaller deeper pan can hold the same volume of water as a larger shallower pan (Fig. 4.2). Ultimately, this process creates a nested series of pans with progressively younger pans developing within the boundaries of older larger pans. At all stages calcrete is formed around the margins of the water body in the pan and older calcrete is left high above the floors of the younger pans forming a bounding calcrete scarp to the depression.

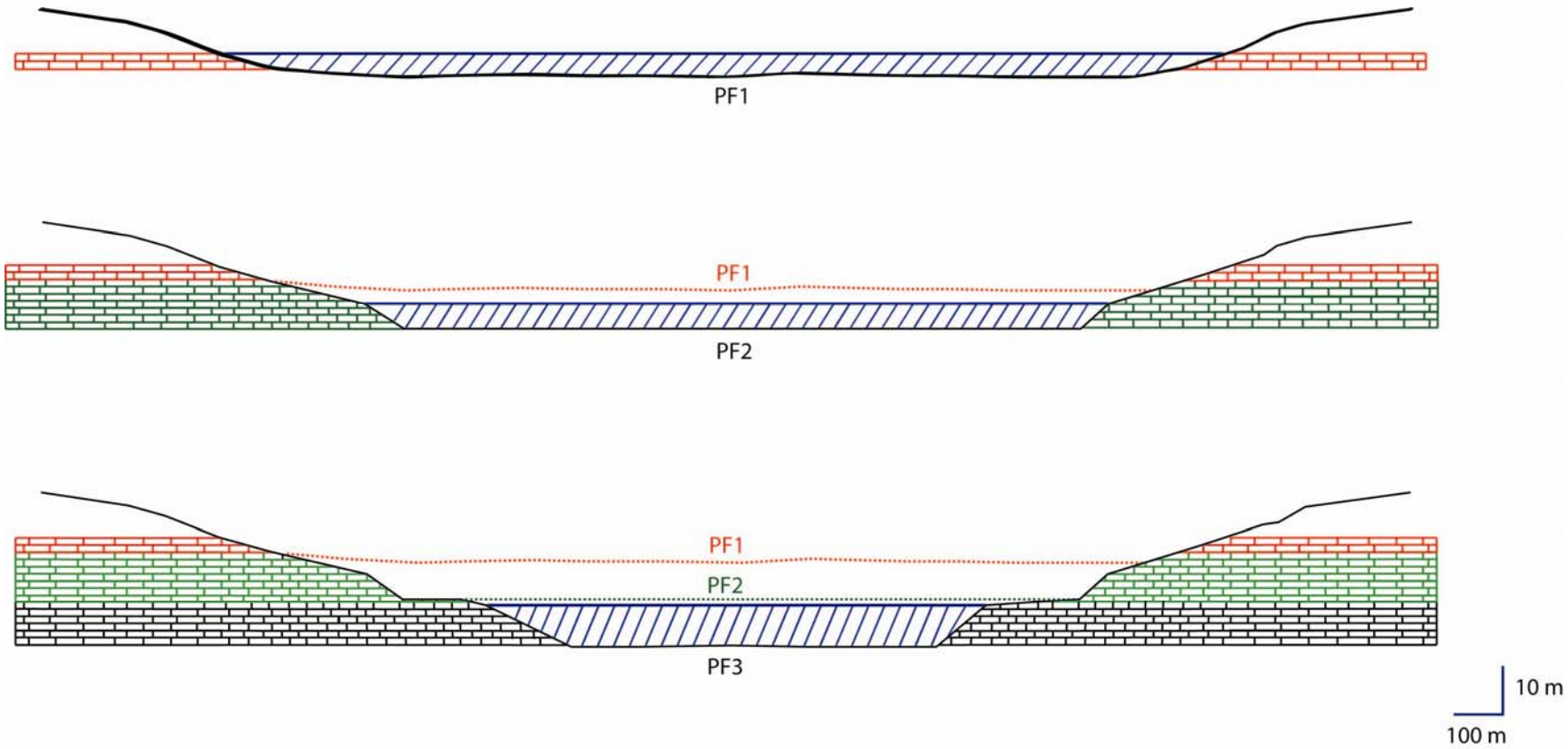

Fig. 4.2 Stages in the development of nested pans and bounding calcrete scarps. During stage 1 (PF1) the diameter of the lake in the pan is 2km and the water depth is 4 m. During stage 2 (PF2) chemical weathering has deepened the pan and reduced the diameter of the lake to 1.5 km. Assuming the volume of water in the lake is the same, the depth of the lake must now be 5.3m. During stage 3 (PF3) the diameter is 1 km and the depth of water is 8 m. Calcrete (brick pattern) has formed around the margins of the pan due evapotranspiration of ground water at each stage in the evolutionary process. Calcrete may also form on the pan floor during particularly severe dry periods but will be re-dissolved and the pan deepened by solution during later intervals of much wetter climate. Old pan floors are shown as red dashed lines. Water levels are shown in blue and lake water is indicated by hatching in blue. The oldest calcrete is in a red brick pattern, intermediate age calcrete is green, and the youngest calcrete is colorless.

CHAPTER 5

PALEOENVIRONMENTAL EVIDENCE FROM THE OTJIMARURU PAN RECORD

This chapter reviews the evidence for environmental/climatic changes at Otjimaruru Pan during the period of record from ca. 80 ka to present.

The OSL Age Data

As mentioned previously in Chapter 3 the OSL ages for the dunes of the Otjimaruru Pan system indicate that accumulation varied considerably over time. Figure 5.1 presents paleoenvironmental data, including sediment granulometry and MS, from the linear dune and inner and outer lunette dunes at Otjimaruru Pan for the last 80 ka. The shore ridge accumulated very rapidly (65cm/ka) reaching a height of over 2m by ca. 2 ka. The sands of the ridge most likely accumulated by wave action during a wet phase and were then modified by wind during a subsequent dry phase lasting from3-2 ka. The linear dune accumulated more or less at a constant rate (8.15cm/ka) during the last 40ka but there is evidence suggesting a slightly increased rate of deposition between 22ka and 11ka (9cm/ka). Both the inner and outer lunettes appear to have accumulated during approximately the same time range but both appear to have accumulated more rapidly at around the same time, from 78-64ka (7.971cm/ka) in the case of the inner lunette and from 75-63 ka (8.62cm/ka) for the outer lunette. In addition, the outer lunette grew more rapidly from 23-17ka (16.13cm/ka), at a time when the linear dune was also growing more rapidly.

These findings suggest more rapid accumulation of dunes in the area from approximately 23 ka-11 ka as well as from 78-63 ka. These periods of increased accumulation, which correspond with isotope stages 4 and 2, suggest that conditions were much drier and certainly much windier than today. The implication is that glacial conditions may have increased sand accumulation on the lunette and linear dunes. The rapid accumulation of the shore ridge in the late Holocene from ca. 3-2 ka suggests that in the past many minor dry intervals were superimposed on this broad picture of aeolian activity.

Variations in Sediment Characteristics

In the following section it is assumed that coarser, better sorted sediments in the linear and lunette dunes correspond to periods of increased aeolian activity while intervals of finer, more poorly sorted sediment correspond to periods of reduced dune activity and increased dune stability.

At approximately 40ka, during OIS 3 there are peaks in fine sediment and poor sorting in the linear and lunette dunes. This peak represents the poorest sorting and finest sediment found for every dune with the exception of the shore ridge. The mean grain size of the peak in the outer lunette is 2.55 phi and the sorting value is 1.43. Corresponding values for the linear dune are 2.35 phi and 1.47, and for the inner lunette dune 2.52 phi and 1.78. This time period also matches a period of reduced dune accumulation in the three dunes, all the evidence suggesting a period of reduced aeolian/dune activity and possibly wetter conditions.

At the time of OIS 2, sediments in the linear dune dating to 22-11ka and in the outer lunette dune dating to 23-17ka are much coarser and better sorted than adjacent sediments. There is a similar coarsening of grain size accompanied by better sorting in the outer lunette at

65ka, during OIS 4. The sediments of the inner lunette are also coarser and better sorted around the same time (78-64 ka). The occurrence of coarser and better sorted sediments in the dunes during OIS 4 and 2 indicates that during these glacial intervals climatic conditions were more conducive to dune building and aeolian activity.

A thin surface sediment layer on the dunes also appears to be coarser and better sorted. This may represent a relatively stable dune surface where fines are deflated leaving coarser material behind as a lag. However, perhaps a more likely explanation is that the coarsening represents overgrazing of the dune crests allowing mobilization of fines that would otherwise be fixed by a cover of vegetation.

A possible explanation for the decrease in fines during glacial periods is that the water body in the pan was more permanent than today. Coupled with stronger winds wave action along the shores of the pan lake would have moved sand alongshore in the downwind direction, producing a shore ridge or beach ridge. Maximum sand accumulation would be in the central sections of the lunette dunes, which represent the maximum sand flow direction. Deflation of the shore ridge during the dry part of the year or during a later drier phase of climate would move the finer sediment onto the inner lunette dune. The rapid accumulation of sand on the lunettes would have been helped by an increase in vegetation cover during the moist lake phase, as vegetation stabilizes the dune surface and traps sand. A vegetation cover also allows winnowing of fines resulting in coarser sands on the dune. During interstadials, a weaker wind system and less frequent flooding would leave the shore ridge less prominent and result in a slower accumulation on the whole.

Variations in MS

Until recently the majority of MS studies were undertaken on the deep loess deposits of the Central Plateau of China. Studies by Heller et al. (1987) and Kukla et al. ((1987, 1991) have demonstrated that MS is an excellent paleoclimate proxy. Variations in MS in the loess deposits correlated strongly with deep ocean core stable isotope records with MS peaks corresponding to interglacial periods and other regional paleoenvironmental proxies. Heller (1991) found that the highest MS vlues corresponded with the most intensely weathered paleosols. In fact, Ellwood et al. (1997) state that "MS variations are attributed to variations in the climate controlled pedogenesis and the magnetic minerals including maghemite". (Balsam, Ellwood and Ji 2005) note that high MS defines conditions that are more conducive to soil development in a given area. This suggests lack of rainfall in the Kalahari as this is the climate variable that currently retards soil development.

In looking at MS variations with depth it is important to realize that the data must be viewed with the understanding that "perfect, undisturbed records" are unlikely. This is because the sampling protocol for the outer lunette, however carefully it was carried out in the field, cannot preclude some, hopefully minor mixing of sediment in the auger hole. Perfect records are also unlikely because dune sands in the Kalahari may be heavily bioturbated(Bateman et al. 2007). It is assumed here that disturbed sections will either show multiple very rapid changes in MS due to sediment mixing or will show long periods when MS changed very little, also due to mixing. Despite these potential problems, the MS records from Otjimaruru appear to provide important information on past climates and conditions.

By far the best MS record is from the outer lunette dune as this record covers 80 ka at an average chronologic resolution of 1.7 ka between samples. The inner lunette also provides an MS

record covering 80ka but includes only five OSL ages and 12 data points as it was not possible to sample for MS at 12 cm intervals because sand did not hold in the auger headl. Although detailed MS sampling was successful in the linear dune, the record only covers 40 ka. Comparison of the three MS records from Otjimaruru is therefore difficult. However, even with the stated limitations the MS data do seem to provide environmental information that is frequently consistent from one record to another, although the outer lunette record is the longest and most detailed and seemingly the least affected by post-depositional disturbance of the sand. For this reason the outer lunette dune record forms the core of the paleoenvironmental information on Otjimaruru presented below.

In the outer lunette record higher MS values appear to correspond to warmer wetter oxygen isotope stages (OIS) also known as marine oxygen isotope stages 1, 3, and 5. Conversely lower MS values appear to correspond to colder, windier, and possibly drier OIS 4 and 2 when soil development was probably retarded. The MS records for the inner lunette and linear dune both show low MS values centered on OIS 2, supporting the outer lunette dune record.

There is a peak in sediment fineness and poor sorting at 4-5ka during OIS 1 found in every dune record, save the shore ridge, that corresponds with a high peak in MS at 5ka. This period may have been a wet phase that immediately preceded the development of the shore ridge. Low MS values during the beginning of OIS 1 and the end of OIS 2 correspond with coarser, better-sorted sediments in these same dunes indicating a drier period during this time. Around 20 ka there is a fining of sediment and poorer sorting in both the linear and outer lunette dunes towards the end of OIS 3 that can be correlated with high MS values in both dunes. During most of OIS 3, MS in the inner and outer lunette dunes is high and corresponds with finer more poorly sorted sediment. At 40 ka MS is low in the outer lunette corresponding with a coarsening of

sediment and better sorting. This may have been a brief dry period in an otherwise wetter-than-present environment. Before 40 ka the only reliable MS record is that from the outer lunette. During OIS 4 MS values from this dune are lower and correspond to better sorted coarser sediment.

MS of sediment from the deeper section o f the linear dune is low compared with MS of the inner and outer lunettes at this time, which are high. A possible explanation for this is that calcrete nodules were encountered near the bottom of the linear dune auger hole. The calcium carbonate in samples taken from these sediments may have affected the MS results.

Summary of Evidence

Periods of more rapid deposition, better sorting, coarser sediment, and lower MS values represent periods of increased aeolian activity, stronger winds and/or drier conditions at Otjimaruru. Periods of slower sediment deposition, poorer sorting, finer mean grain size, and higher MS values represent periods of increased dune stability and weaker winds and/or wetter conditions at Otjimaruru. From 78-63 ka, during OIS 4 the dunes around Otjimaruru were active and the environment was likely windier and drier than present. From 63-23 ka, during most of OIS 3 the data indicate that winds were less powerful, the environment was wetter, and the dunes were generally more stable. Around 23ka and during OIS 2 the climate at Otjimaruru was drier and windier until at least 17 ka and possibly until 11 ka. From 11-3 ka the climate of the region was wetter and the winds weaker. During this early Holocene wet period, water in Otjimaruru Pan moved sand alongshore. This sand was later reworked by wind from 3-2 ka to form a shore ridge around the downwind margin of the pan. The sand is light colored because while in the water the iron was largely removed.

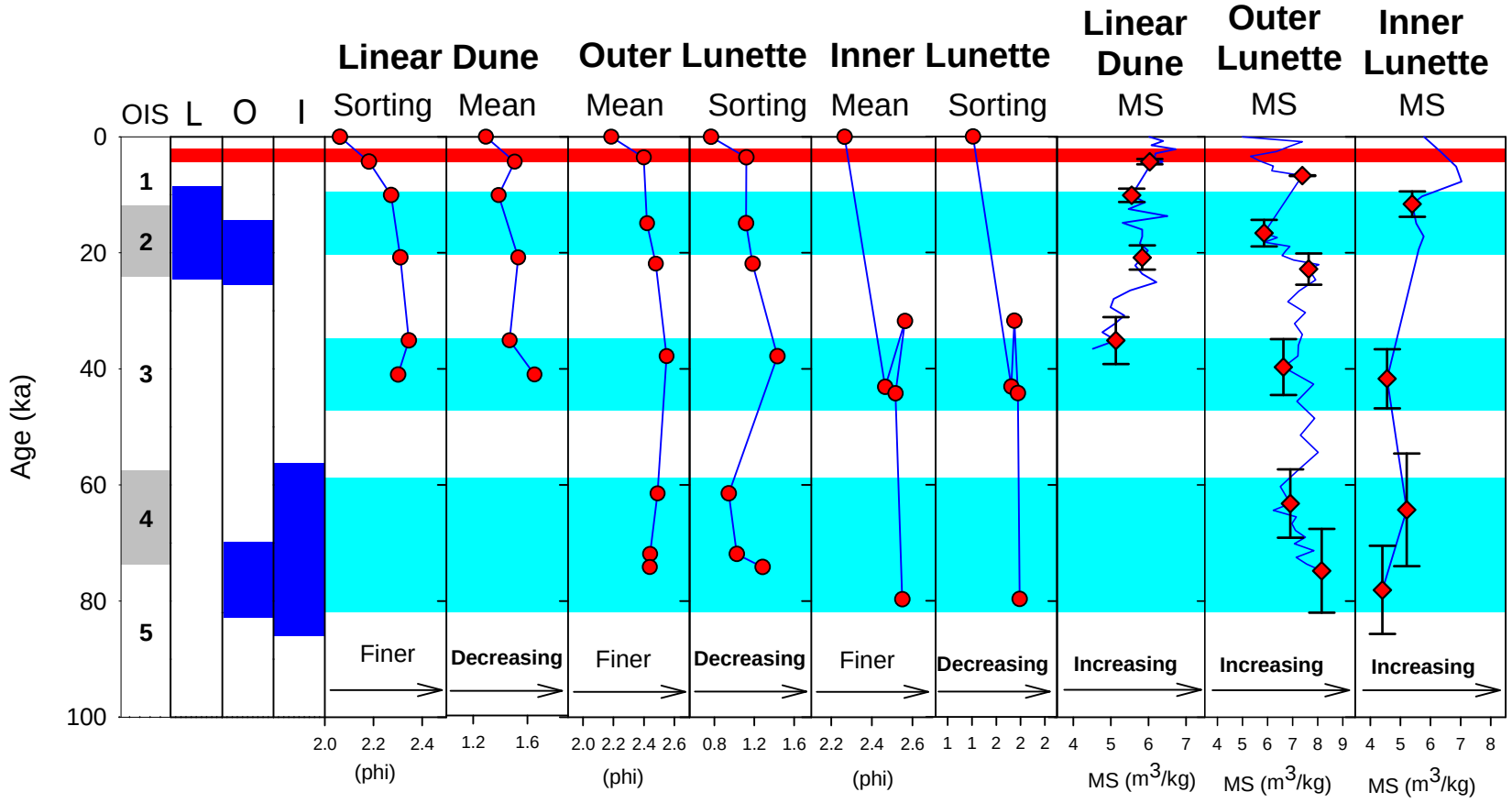

Fig. 5.1 Mean grain size, sorting and MS of linear dune and inner and outer lunette dune sediments. The red line shows the age of the shore ridge (3.4-2.1 ka), which may record a drier and windier climate. The dark blue boxes show periods of more rapid deposition on the linear (L), outer lunette (O) and inner lunette (I) dune. The light blue boxes show periods of lower MS, poorer sorting, and finer grain size in the dunes that suggest increased aridity and windier conditions. OIS stages are shown in the far left column. The OSL ages are shown as red diamonds with error bars plotted in the MS columns.

Chapter 6

DISCUSSION

In this chapter the paleoenvironmental record from Otjimaruru is compared to both regional and global climate records and possible explanations for the changes are presented.

Comparison of the Otjimaruru Record with other Regional Records of Climate Change

Chronological Issues

The most detailed proxy record of past climate for Otjimaruru Pan is contained in the MS records from the four dunes, particularly the record from the outer lunette dune. However, correlating this MS time series with other regional records of climate change must take into account uncertainties in the chronologies for the records being compared. The chronologies for the Otjimaruru MS record, and chronologies for several regional records going back to ca. 75 ka, are based on OSL ages with an uncertainty of about ± 10%. Several other studies have employed radiocarbon dating but where this is used to date carbonate it is rare to find that the ages were corrected for the incorporation of old carbon into the deposit and so the ages are likely to be too old, possibly a great deal too old. Radiocarbon dating has also been used to date marine cores within the age range of the method (ca. 45 ka). The resulting chronologies are extended by comparing the marine core isotope record with other such records from better-dated cores and adjusting the chronology accordingly. Perhaps the most reliable chronologies available are

uranium-series chronologies for cave speleothems because this method provides ways of checking for possible contamination by thorium, which would produce ages that are much older than the true ages.

Long Regional Records

Figure 6.1 shows the most important regional paleoclimate records that extend to ca. 80 ka. In addition, the figure includes the Taylor Dome ice core oxygen isotope record. Despite the chronological and other problems mentioned above, the records from other sites in the region share many similarities with the MS records from the Otjimaruru dunes. For example, sediment evidence from White Paintings rock shelter (WPS) indicates eleven phases of greater surface stability in the shelter that were accompanied by weak soil formation (Ivester et al. 2010). These periods are evidenced by buried soil A-horizons dated by OSL to ca. 2.5, 5-7.5, 15, 25-26, 31, 36, 47-51, 58-60, 65-73, 97, and 115 ka (Fig. 6.1.D). The ages of lake high-stands in the Makgadikgadibasin of Botswana at 8.5 ± 0.2, 17.1 ± 1.6, 26.8 ± 1.2, 38.7 ± 1.8, 64.2 ± 2.0, 92.2 ± 1.5, and 104.6 ± 3.1 ka (Fig. 6.1.E) (Burrough and Thomas 2008, Burrough et al. 2009b) correspond closely with the wet intervals at White Paintings rock shelter. In addition, evidence from Tsodilo Hills in NW Botswana (Fig. 6.1.A) indicates the presence of a small lake in the past that is not present today. Luminescence ages for shore sediments indicate the existence of a small lake ca.12-13 ka and 18 ka. In addition, calibrated AMS radiocarbon ages for freshwater mollusc shells found within lacustrine marls (not corrected for old carbon) point to high lake phases ca. 14-17, 23, 32, and 36 ka(Robbins et al. 1998, Thomas et al. 2003). Together, the OSL and AMS radiocarbon ages define five lake intervals that match with the timing of high MS values in the Otjimaruru dune sands.

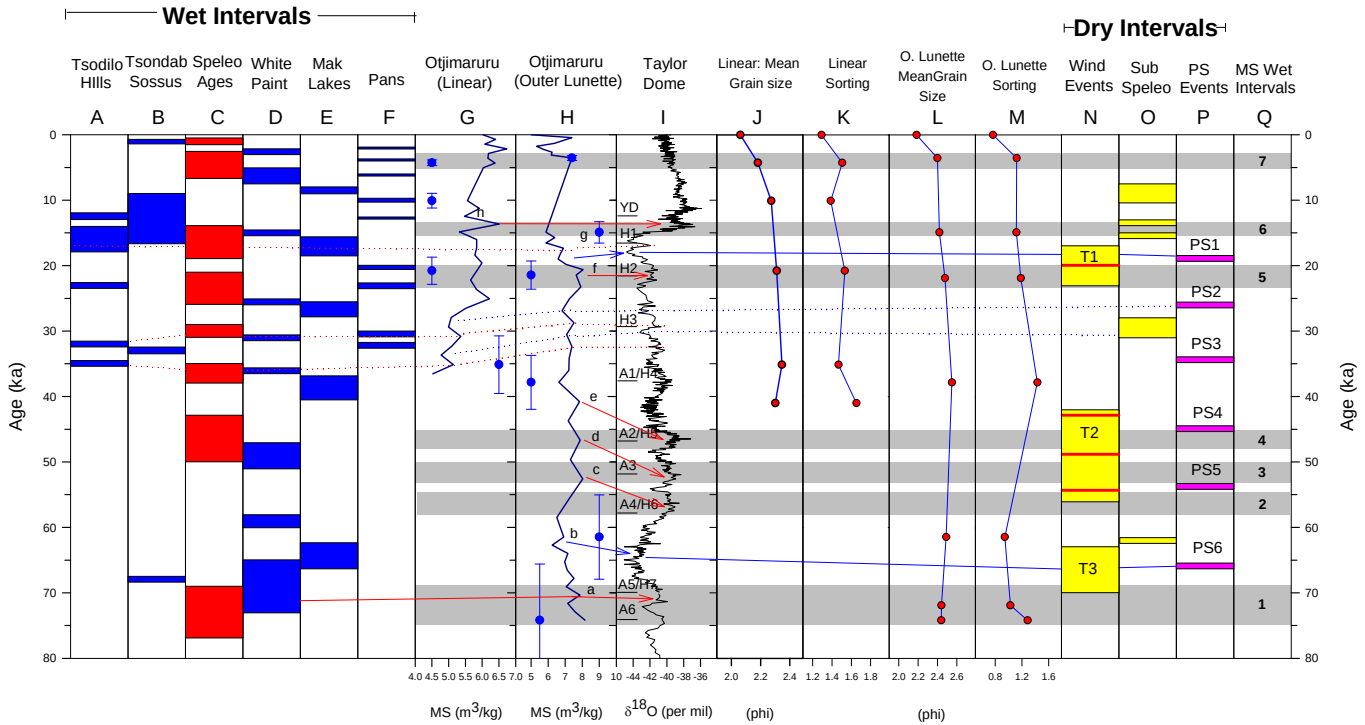

Fig. 6.1 Otjimaruru Pan grain size and MS records compared with other regional and global paleoclimate records. (modified after Brook et al. manuscript in prep.) Columns A-F show wet phases of climate and columns N-P dry/windier phases. A: freshwater mollusc and lake sediment ages for Tsodilo Hills, Botswana, B: fluvial sediments at Tsondab and Sossus Vlei, C: speleothem ages for Botswana, D: paleosols at White Paintings Rock Shelter, Tsodilo Hills, Botswana E: periods of beach ridge formation at Makgadikgadi Pan, Botswana, F: wet intervals at Etosha Pan, Namibia, Witpan, South Africa, and Urwi Pan, Botswana, G: Otjimaruru linear dune MS variations, H: Otjimaruru outer lunette dune MS variations, I: Antarctic ice core record from Taylor Dome with the Younger Dryas (YD), Heinrich events (H1-H7) and Antarctic warm periods (A1-A6) indicated, J&K: Otjimaruru linear dune mean grain size and sorting, L&M: Otjimaruru outer lunette dune mean grain size and sorting, N: periods of trade wind enhancement, T events (yellow) with peaks shown in red, S. Atlantic marine core GeoB 1023-5, O: submerged speleothems from cenotes in NE Namibia, P: N. *pachiderma* (s) or PS events in ocean core GeoB1711 off the coast of Namibia, Q: Interpreted wet periods (grey). In columns G and H OSL ages and error bars are indicated. Red (a, c, d, e, f, and h) and blue (b and g) lines show possible correlations (solid = more certain; dotted = less certain) between records of wet and dry intervals.

Variations in the frequency of speleothem and tufa ages from the summer rainfall zone of Southern Africa indicate peak wetness at 77-69, 48-46, 37-36, 31-30, 27-26, 24-23, 16-15, 12.5-11, and 8.2-7.9 ka (Fig. 6.1.C) (Brook et al. 1997, Brook, Cowart and Brandt 1998). During the middle and late Holocene the data indicate more moisture at 6.9-2.6 and 1.6-0.5 ka with peak wetness at 4.5 ka and 1.5 ka(Brook et al., 1998).

Several other pans in the area have provided information on wetter phases of climate during the last ca. 40 ka (Fig. 6.1.F). OSL ages for pan floor sediments at Witpan in southern Namibia suggest lake conditions at ca 32 ka and 20ka (Telfer et al. 2009). Phytoliths in the sands of the innermost lunette dune at Witpan suggest wetter conditions at 2.1 ka, while reduced activity of the nearby linear dunes indicates wetter conditions at 15-19 ka and 21-27 ka(Telfer and Thomas 2007). OSL ages for shorelines around the western margin of Etosha Pan in northern Namibia suggest wetter, lake conditions in the pan at ca. 6.4, 4, and 2.1 ka(Brook et al. 2007). In addition, radiocarbon ages for organic material in stromatolites from Urwi Pan in Botswana indicate wetter conditions ca. 12.8-12.6 ka and 10.2-9.8 ka(Brook, unpublished data, 2011). At Aminuis Pan only 15 km NNE of Otjimaruru Pan, OSL ages on old pan floor deposits indicate wetter conditions at 27.43±2.95 to 20.80±2.24ka, and at 8.58±0.74 ka (Brook et al., manuscript in prep.).

Evidence of drier conditions during the last 80ka also matches the Otjimaruru dune MS records of climate events. For example, U-series ages of submerged speleothems in flooded caves and cenotes in NE Namibia, recovered by divers from depths of 3-40 m below modern ground water levels, indicate periods of lower ground water table and therefore much drier conditions 7.5-10.6, 13.5, 15.4, 28-31, 62, and 107-112 ka (Fig. 6.1. O) (Brook et al. 1998).

Pollen influx data from South Atlantic marine core GeoB 1023-5 (Fig. 6.1.N) reveal three periods (T1-T-3) during the last 80 ka with strong Southeast Trade winds at ca. 16-23, 42-55, 63-70, 86-93, and 105-109 ka(Shi 2001). These periods may also have been characterized by increased aridity. The pollen data record stronger trade winds at 109-105 (T5), 92-86 (T4), 70-63 (T3), 56-42 (T2) and 23-17 ka (T1). However, during T2 the most prominent peaks in pollen influx were at 54, 49, and 43 ka and during T1 the single peak was at 20 ka.

Little et al. (1997) have identified six N. *pachyderma* (s) or PS events in marine core GeoB 1711 off the Namibian coast (PS1-PS9) in the last 135 ka when the percentage of the cold-water foraminifer N. *pachyderma* (s) increased substantially (Fig. 6.1.P). Shi et al. (2001) adjusted the chronology presented by Little et al. (1997) using additional age data. PS events are thought to indicate increased upwelling of the Benguela Current in the Southeast Atlantic triggered by stronger Southeast Trade winds. Periods of high abundance of *N. pachyderma* (s) (PS events) may be recording increased intensity and zonality of the SE trade winds controlling the Benguela upwelling system off the coast of Namibia.According to Little et al. (1997), the timing of the PS events is: PS6 = 71-65 ka, PS5 = 53 ka, PS4 = 42.4 ka, PS3 = 36.7-32.7 ka, PS2 = 29-26.1 ka and PS1 = 21.7-19.2 ka. Note that the values used in Figure 6.1 (column P) are PS1-PS5: 19, 27, 34, 45, and 54 ka following Shi et al.(2001).

Water-lain sediments in the interdune areas near and associated with the former course of the Tsondab River in Namibia have been OSL dated to reveal a wet phase in climate from 17-10ka. At Hartmut Pan, ages on silty mud units showed deposition at 16.9±0.9 ka and 13.0±1.0 ka. Mud units at Ancient Tracks were younger dating to 12.0±0.7, 12.8±0.8, 11.5±0.5, and 10.5±0.5 ka(Stone, Thomas and Viles 2010). At SossusVlei in the Namib Sand Sea, fluvial deposits in interdune areas beyond the present end point of the Tsauchab River, indicate that the

river flowed further into the desert at c. 25ka, 9-7 ka, and 0.9-0.3 ka(Brook, Srivastava and Marais 2006).

Regional Correlations

Comparison of the MS data from Otjimaruru with the better-dated $\delta^{18}O$ record for Taylor Dome in the Antarctic shows considerable agreement between peaks in MS and peaks in $\delta^{18}O$. Because of this, the Taylor Dome record of climate changes, with high $\delta^{18}O$ indicating warmer temperatures and low $\delta^{18}O$ recording colder temperatures, was used as a base for the discussion that follows. Fig. 6.1 shows that the regional paleoenvironmental data do not always agree on the exact timing of wet and dry periods in the past. This is most likely because of chronological problems introduced by large uncertainties in ages and sometimes unreliability of evidence (Chase and Meadows 2007). However, of the records shown in Fig. 6.1, the most reliable chronologically are the speleothem records (Fig. 6.1.C & O). This is because the speleothems in the records were dated using uranium-series methods and so are far more reliable than the records in Fig. 6.1 that are based on radiocarbon or OSL chronologies. For this reason more emphasis is given to correlations between the Otjimaruru, Taylor Dome, and speleothem records than is the case for the other records shown where the ages indicated may be slightly offset from the true ages.

The Otjimaruru MS data suggest seven wet climatic intervals (numbered 1-7 in Fig. 6.1.Q) in the last 75 ka centered on ca. 72, 56, 51, 47, 22, 14, and 4 ka. In addition, in the interval 45-23 ka there are several minor peaks in MS that may record other wet intervals such as at ca. 32 ka and 29 ka, which approximately correspond with wet intervals in the speleothem record (Fig. 6.1.C) and in data from Tsodilo Hills in NW Botswana (Fig. 6.1.A). The small peak in MS

at ca. 17 ka may also record a wet interval as this peak correlates well with evidence of wetter conditions in the records for Makgadikgadi Pan, White Paintings rock shelter, Tsondab and SossusVlei, and the Tsodilo Hills, as well as the record of periods of speleothem deposition. These possible wet intervals, and linkages between records, are shown in Fig. 6.1. by dotted red lines.

MS wet interval 1 (MS1) correlates with the speleothem, White Paintings rock shelter and Tsondab/Sossus evidence (Fig. 6.1. B, C, D) of wet conditions at this time. MS2 correlates with the speleothem data, while MS3 and MS4 correlate with the speleothem and White Paintings data. MS5 and MS6 correlate with separate wet intervals suggested by the speleothem data (Fig. 6.1.C) as well as with wet intervals at Tsodilo Hills. MS5 also matches evidence from pans of wetter conditions in the region (Fig. 6.1.F). MS6 correlates reasonably well with wet intervals in the Makgadikgadi, White Paintings, and Tsondab and SossusVlei records (Fig. 6.1.B, D, E). The most recent wet interval, MS7, centered at 4 ka, correlates with evidence of increased moisture in the speleothem, White Paintings, and pan records.

Periods of low MS that are evidence of dry intervals of climate, correlate with the timing of major wind events, with deposition of now-submerged speleothems, and with PS events (Fig. 6.1.N, O, P). There are two prominent periods with low MS at ca. 65 ka and 16 ka that are identified in Fig. 6.1 by blue lines. These low MS periods correlate with the T1 and T3 wind events and the PS1 and PS6 events. In the period 45-23 ka there were several periods with low MS that may record additional dry intervals of climate. These are indicated in Fig. 6.1 with a dotted blue line, which links the supporting data. The first is at ca. 30 ka and correlates with the deposition of speleothems that are now submerged. The second interval is centered on ca. 26 ka and correlates with the PS2 event.

Correlations with the Antarctic Taylor Dome Isotope Record and with Heinrich and Antarctic Warm Events.

The Otjimaruru MS records provide a reasonably similar record of climate changes to that of the Antarctic Taylor Dome ice core isotope record, with higher $\delta^{18}O$ values (warmer) corresponding to higher MS values (wetter). Some possible correlations between the two records are shown in Fig. 6.1. For example, at 17.5 ka (OIS 2) and at 65 ka (OIS 4) the records indicate colder and drier conditions (low $\delta^{18}O$ and low MS, respectively), while at 22 ka they indicate warmer and wetter conditions (high $\delta^{18}O$ and high MS, respectively).

Significantly, matching peaks in MS (Otjimaruru) and $\delta^{18}O$ (Taylor Dome) correlate strongly with Heinrich (H) and Antarctic Warm (A) events (Fig. 6.1) (Blunier 2001). For example H2 correlates with peaks in MS and $\delta^{18}O$ with low values in both variables a few thousand years before and after. In fact, with the exception of H1, H3, and A1/H4, every H/A event correlates with a wet interval in Fig. 6.1 when the MS and $\delta^{18}O$ data suggest warmer and wetter conditions than present. Furthermore, H1 and H3 correlate with possible wet periods indicated in Fig. 6.1.

The correlation between high MS and Otjimaruru and high $\delta^{18}O$ at Taylor Dome suggests that warm conditions in the southern oceans bring increased moisture to Southern Africa. While Heinrich events are associated with colder periods in the North Atlantic, they bring warmer conditions to the South Atlantic (Blunier 2001). Heinrich events disrupt the thermohaline oceanic conveyer belt in the Atlantic by altering the salinity of the North Atlantic Ocean (Stocker 1998). This reduces the flow of warm water to the North Atlantic trapping it in the South Atlantic and thus creating a "bipolar see-saw" where the north gets colder and the south becomes

warmer (Stocker 1998, Seidov and Maslin 2001). Abrupt warm periods are followed by century long cooling periods at an average interval of approximately 2000 years (Seidov and Maslin 2001). This causes the South Atlantic to warm significantly resulting in a weakened South Atlantic anticyclone and a weakened South African Anticyclone. The weakening of these two high pressure systems, coupled with warmer Southern Hemisphere oceans, appears to bring more moisture to Southern Africa during H/A events (Blunier 2001).

Summary

Bateman et al. (2007) have argued that a possible explanation for the lack of structure in Kalahari dunes is that structures have been lost due to post-depositional disturbance or bioturbation. The MS data from the Otjimaruru dunes show that this may not always be the case. Although there may be some disturbance of the sediment by biological activity, structure appears to have been preserved sufficiently for an MS record to be obtained. Clearly the Otjimaruru data indicate that long and possibly quite detailed paleoenvironmental records are possible by the study of age, MS, and sediment texture of lunette and liner dunes in the Kalahari Desert.

The paleoenvironmental record derived from the Otjimaruru pan-lunette system correlates reasonably well with the regional and global paleoclimate proxies shown in Fig. 6.1. High MS intervals appear to match wet intervals at other sites while low MS intervals match dry periods. The Otjimaruru outer lunette MS record, correlates with the Taylor Dome Antarctic ice core $\delta^{18}O$ isotope record and with Heinrich and Antarctic warm events. High MS correlates with high $\delta^{18}O$ indicating that at these times conditions were warmer and wetter than present in the South Atlantic Ocean and in Southern Africa.

The Otjimaruru MS record suggests that there were at least seven major wet intervals in the last 75 ka, centered on ca. 72, 56, 51, 47, 22, 14, and 4 ka, with three other less well defined wet periods at ca. 32, 29, and 17 ka. Low MS values suggest at least two major dry periods centered at ca. 65 ka and 16 ka as well as possible dry periods at ca. 30 ka and 26 ka. These findings indicate that pans and their associated lunettes and linear dunes can provide accurate paleoclimate records for the region.

CHAPTER 7

CONCLUSIONS

This study has provided new information on the paleoclimates of the Southern Kalahari Desert and has also produced evidence of the origin and evolution of the pan-lunette systems in this area. The research produced the following specific findings.

1. The pan-lunette systems of the Southern Kalahari originated prior to 80ka as evidenced by the oldest age obtained for the lunette dunes at Otjimaruru Pan.
2. The morphology, sediment, and age characteristics of the linear and lunette dunes at Otjimaruru suggest that the pan formed within a pre-existing field of linear dunes by local flooding of low-lying interdune areas during wetter periods of climate. At these times wind and wave action eroded the linear dunes moving sand downwind to form lunette dunes. The outer lunette dune at Otjimaruru is formed from the pre-existing linear dunes south of the pan. The inner lunette was formed by sand that migrated across the pan in water before being blown into the lunette system by strong winds. The lunettes continue to form today.
3. The dunes at Otjimaruru appear to have accumulated more rapidly during OIS 2 and 4 suggesting that these were times with much stronger winds and possibly also drier climate.
4. Kalahari linear dune sand textural characteristics have previously provided little information on past climates but the Otjimaruru data reveal deposition of coarser and

better sorted sediments during OIS 2 and 4 indicating that dune sands do vary in nature with climate.

5. The lack of structure in Kalahari dunes has led some (e.g. Bateman et al., 2007) to argue that they do not contain reliable paleoclimatic data because of extensive bioturbation by animals and plants. However, MS data from the linear and lunette dunes at Otjimaruru appear to record climatic shifts from wet (stable dunes) to dry (unstable dunes) with MS peaking during wet, stable dune periods, when weak soil formation was possible.
6. The higher-resolution MS data from the Otjimaruru dunes correlate well with regional climate proxy records and with Antarctic ice core stable isotope data.
7. Correlations between MS peaks and Heinrich/Antarctic Warm events suggests that warmer southern oceans at these times reduced SE trade wind velocities and brought more rainfall to the Southern Kalahari resulting in more stable dunes and weak soil development.

The research findings summarized above are significant because they provide a new model for the origin and evolution of Southern Kalahari pan-lunette systems and for the first time show that these systems are much older than ca. 80 ka. The new model suggests that both water and wind have been critical in the formation of the pan-lunette systems and that their stability in the landscape is due to frequent climate shifts with no prolonged dry intervals that would allow re-establishment of the linear dune systems across the pans. Particularly significant is the finding that both linear and lunette dunes preserve a record of past climates in the MS of the sediments with high MS recording periods of wetter climate, increased dune stability, and possibly also more frequent and more prolonged flooding of the pans. This means that the

Kalahari dunes may preserve very long records of climate conditions if samples can be recovered from the tops to the bases of the dunes.

REFERENCES

Aitken, M. J. 1985. *Thermoluminescence dating*.

BÃ¸tter Jensen, L. (1999) Blue light emitting diodes for optical stimulation of quartz in retrospective dosimetry and dating. *Radiation protection dosimetry,* 84**,** 335.

Balsam, W., B. Ellwood & J. Ji (2005) Direct correlation of the marine oxygen isotope record with the Chinese Loess Plateau iron oxide and magnetic susceptibility records. *Palaeogeography, Palaeoclimatology, Palaeoecology,* 221**,** 141-152.

Bateman, M. D., C. H. Boulter, A. S. Carr, C. D. Frederick, D. Peter & M. Wilder (2007) Preserving the palaeoenvironmental record in Drylands: Bioturbation and its significance for luminescence-derived chronologies. *Sedimentary Geology,* 195**,** 5-19.

Bateman, M. D., D. S. G. Thomas & A. K. Singhvi (2003) Extending the aridity record of the Southwest Kalahari: current problems and future perspectives. *Quaternary International,* 111**,** 37-49.

Blott, S. J. & K. Pye. 2001. GRADISTAT: a grain size distribution and statistics package for the analysis of unconsolidated sediments. 1237-1248. John Wiley & Sons, Ltd.

Blunier, T. (2001) Timing of millennial-scale climate change in Antarctica and Greenland during the last glacial period. *Science,* 291**,** 109.

Bowler, J. M. (1973) Clay Dunes: Their occurrence, formation and environmental significance. *Earth-Science Reviews,* 9**,** 315-338.

--- (1986) Spatial variability and hydrologic evolution of Australian lake basins: Analogue for pleistocene hydrologic change and evaporite formation. *Palaeogeography, Palaeoclimatology, Palaeoecology,* 54**,** 21-41.

Brook, G. A., J. B. Cowart & S. A. Brandt (1998) Comparison of Quaternary environmental change in eastern and southern Africa using cave speleothem, tufa and rock shelter sediment data. *Quaternary Deserts and Climatic Change***,** p. 239-249.

Brook, G. A., J. B. Cowart, S. A. Brandt & L. Scott (1997) Quaternary climatic change in southern and eastern Africa during the last 300 ka: the evidence from caves in Somalia and the Transvaal region of South Africa. *Zeitschrift für Geomorphologie* 108: 15-48.

Brook, G. A., E. Marais, P. Srivastava & T. Jordan (2007) Timing of lake-level changes in Etosha Pan, Namibia, since the middle Holocene from OSL ages of relict shorelines in the Okondeka region. *Quaternary International,* 175**,** 29-40.

Brook, G. A., P. Srivastava & E. Marais (2006) Characteristics and OSL minimum ages of relict fluvial deposits near Sossus Vlei, Tsauchab River, Namibia, and a regional climate record for the last 30 ka. *Journal of Quaternary Science,* 21**,** 347-362.

Bullard, J. E., D. S. G. Thomas, I. Livingstone & G. S. F. Wiggs (1997) Dunefield Activity and Interactions with Climatic Variability in the Southwest Kalahari Desert. *Earth Surface Processes and Landforms,* 22**,** 165-174.

Burrough, S. L. & D. S. G. Thomas (2008) Late Quaternary lake-level fluctuations in the Mababe Depression: Middle Kalahari palaeolakes and the role of Zambezi inflows. *Quaternary Research,* 69**,** 388-403.

Burrough, S. L., D. S. G. Thomas & R. M. Bailey (2009a) Mega-Lake in the Kalahari: A Late Pleistocene record of the Palaeolake Makgadikgadi system. *Quaternary Science Reviews,* 28**,** 1392-1411.

Burrough, S. L., D. S. G. Thomas & J. S. Singarayer (2009b) Late Quaternary hydrological dynamics in the Middle Kalahari: Forcing and feedbacks. *Earth-Science Reviews,* 96**,** 313-326.

Chase, B. (2009) Evaluating the use of dune sediments as a proxy for palaeo-aridity: A southern African case study. *Earth-Science Reviews,* 93**,** 31-45.

Chase, B. M. & S. Brewer (2009) Last Glacial Maximum dune activity in the Kalahari Desert of southern Africa: observations and simulations. *Quaternary Science Reviews,* 28**,** 301-307.

Chase, B. M. & M. E. Meadows (2007) Late Quaternary dynamics of southern Africa's winter rainfall zone. *Earth-Science Reviews,* 84**,** 103-138.

Chase, B. M. & D. S. G. Thomas (2007) Multiphase late Quaternary aeolian sediment accumulation in western South Africa: Timing and relationship to palaeoclimatic changes inferred from the marine record. *Quaternary International,* 166**,** 29-41.

Chen, X. Y. (1995) Geomorphology, stratigraphy and thermoluminescence dating of the lunette dune at Lake Victoria, western New South Wales. *Palaeogeography, Palaeoclimatology, Palaeoecology,* 113**,** 69-86.

Ellwood, B. B., K. M. Petruso, F. B. Harrold & J. Schuldenrein (1997) High-Resolution Paleoclimatic Trends for the Holocene Identified Using Magnetic Susceptibility Data from Archaeological Excavations in Caves. *Journal of Archaeological Science,* 24**,** 569-573.

Gee, G. W. 1986. *Particle-size analysis*

Methods of soil analysis. Part 1. Physical and mineralogical methods.

Goudie, A. S. (1989) Wind erosion in deserts. *Proceedings of the Geologists' Association,* 100**,** 83-92.

Goudie, A. S. & G. L. Wells (1995) The nature, distribution and formation of pans in arid zones. *Earth-Science Reviews,* 38**,** 1-69.

Grove, A. T. (1969) Landforms and Climatic Change in the Kalahari and Ngamiland. *The Geographical Journal,* 135**,** 191-212.

Heller, F., X. Liu, T. Liu & T. Xu (1991) Magnetic susceptibility of loess in China. *Earth and planetary science letters,* 103**,** 301-310.

Holmes, P. J., M. D. Bateman, D. S. G. Thomas, M. W. Telfer, C. H. Barker & M. P. Lawson. 2008. A Holoceneâ€"late Pleistocene aeolian record from lunette dunes of the western Free State panfield, South Africa. In *Holocene*, 1193-1205. Sage Publications, Ltd.

Ivester, A. H., G. A. Brook, L. H. Robbins, A. C. Campbell, M. L. Murphy & E. and Marais (2010) A sedimentary record of environmental change at Tsodilo Hills White Paintings Rock Shelter, Northwest Kalahari Desert, Botswana. *Palaeoecology of Africa* 30**,** pp. 53-78.

Kukla, G. (1987) Loess stratigraphy in central China. *Quaternary Science Reviews,* 6**,** 191-207, 209-219.

Lancaster, I. N. (1978) The Pans of the Southern Kalahari, Botswana. *The Geographical Journal,* 144**,** 81-98.

Lancaster, N. (1981) Paleoenvironmental implications of fixed dune systems in Southern Africa. *Palaeogeography, Palaeoclimatology, Palaeoecology,* 33**,** 327-346.

--- (1989) Late Quaternary paleoenvironments in the southwestern Kalahari. *Palaeogeography, Palaeoclimatology, Palaeoecology,* 70**,** 367-376.

--- (1990) Palaeoclimatic evidence from sand seas. *Palaeogeography, Palaeoclimatology, Palaeoecology,* 76**,** 279-290.

Lawson, M. P. & D. S. G. Thomas (2002) Late Quaternary lunette dune sedimentation in the southwestern Kalahari desert, South Africa: luminescence based chronologies of aeolian activity. *Quaternary Science Reviews,* 21**,** 825-836.

Leistner, O. A. & M. J. A. Werger (1973) Southern Kalahari Phytosociology. *Vegetatio,* 28**,** 353-399.

Levin, N., H. Tsoar, L. P. Maia, V. C. Sales & H. Herrmann (2007) Dune whitening and inter-dune freshwater ponds in NE Brazil. *CATENA,* 70**,** 1-15.

Little, I. G., R. R. Schneider, D. Kroon, B. Price, C. P. Summerhayes & M. Segl (1997) Trade wind forcing of upwelling, seasonality, and Heinrich events as a response to sub-Milankovitch climate variability. *Paleoceanography* 12**,** 568-576.

Marker, M. E. & P. J. Holmes (1995) Lunette dunes in the northeast Cape, South Africa, as geomorphic indicators of palaeoenvironmental change. *CATENA,* 24**,** 259-273.

Markey, B. G. (1997) A new flexible system for measuring thermally and optically stimulated luminescence. *Radiation measurements,* 27**,** 83.

McMichael, R. D., U. Atzmony, C. Beauchamp, L. H. Bennett, L. J. Swartzendruber, D. S. Lashmore & L. T. Romankiw (1992) Fourfold anisotropy of an electrodeposited Co/Cu compositionally modulated alloy. *Journal of Magnetism and Magnetic Materials,* 113**,** 149-154.

Murray, A. S. (2000) Luminescence dating of quartz using an improved single-aliquot regenerative-dose protocol. *Radiation measurements,* 32**,** 57.

O'Connor, P. W. & D. S. G. Thomas (1999) The Timing and Environmental Significance of Late Quaternary Linear Dune Development in Western Zambia. *Quaternary Research,* 52**,** 44-55.

Partridge, T. C. & R. R. Maud (1987) Geomorphic evolution of southern Africa since the Mesozoic. *South African Journal of Geology,* 90**,** 179-208.

Prescott, J. R. (1994) Cosmic ray contributions to dose rates for luminescence and ESR dating: large depths and long-term time variations. *Radiation measurements,* 23**,** 497.

Robbins, L. H., M. L. Murphy, A. C. Campbell, G. A. Brook, D. M. Reid, K. A. Haberyan & W. S. Downey (1998) Test Excavations and Reconnaissance Palaeoenvironmental Work at Toteng, Botswana. *The South African Archaeological Bulletin,* 53**,** 125-132.

Seidov, D. & M. Maslin (2001) Atlantic ocean heat piracy and the bipolar climate see-saw during Heinrich and Dansgaard–Oeschger events. *Journal of Quaternary Science,* 16**,** 321-328.

Shi, N. (2001) Southeast trade wind variations during the last 135 kyr: evidence from pollen spectra in eastern South Atlantic sediments. *Earth and planetary science letters,* 187**,** 311.

Singletary, S. J., R. E. Hanson, M. W. Martin, J. L. Crowley, S. A. Bowring, R. M. Key, L. V. Ramokate, B. B. Direng & M. A. Krol (2003) Geochronology of basement rocks in the Kalahari Desert, Botswana, and implications for regional Proterozoic tectonics. *Precambrian Research,* 121**,** 47-71.

Stocker, T. F. (1998) The seesaw effect. *Science,* 282**,** 61.

Stokes, S., G. Haynes, D. S. G. Thomas, J. L. Horrocks, M. Higginson & M. Malifa (1998) Punctuated aridity in southern Africa during the last glacial cycle: The chronology of linear dune construction in the northeastern Kalahari. *Palaeogeography, Palaeoclimatology, Palaeoecology,* 137**,** 305-322.

Stokes, S. & D. S. G. Thomas (1997) Multiple episodes off aridity in southern Africa since the last interglacial period. *Nature,* 388**,** 154.

Stone, A. E. C. & D. S. G. Thomas (2008) Linear dune accumulation chronologies from the southwest Kalahari, Namibia: challenges of reconstructing late Quaternary palaeoenvironments from aeolian landforms. *Quaternary Science Reviews,* 27**,** 1667-1681.

Stone, A. E. C., D. S. G. Thomas & H. A. Viles (2010) Late Quaternary palaeohydrological changes in the northern Namib Sand Sea: New chronologies using OSL dating of interdigitated aeolian and water-lain interdune deposits. *Palaeogeography, Palaeoclimatology, Palaeoecology,* 288**,** 35-53.

Swan, D., J. J. Clague & J. L. Luternauer (1978) Grain-size statistics I; Evaluation of the Folk and Ward graphic measures. *JOURNAL OF SEDIMENTARY RESEARCH,* 48**,** 863-878.

Telfer, M. W. & D. S. G. Thomas (2006) Complex Holocene lunette dune development, South Africa: Implications for paleoclimate and models of pan development in arid regions. *Geology,* 34**,** 853-856.

Telfer, M. W. & D. S. G. Thomas (2007) Late Quaternary linear dune accumulation and chronostratigraphy of the southwestern Kalahari: implications for aeolian palaeoclimatic reconstructions and predictions of future dynamics. *Quaternary Science Reviews,* 26**,** 2617-2630.

Telfer, M. W., D. S. G. Thomas, A. G. Parker, H. Walkington & A. A. Finch (2009) Optically Stimulated Luminescence (OSL) dating and palaeoenvironmental studies of pan (playa) sediment from Witpan, South Africa. *Palaeogeography, Palaeoclimatology, Palaeoecology,* 273**,** 50-60.

Thomas, D. S. G. (1984) Ancient Ergs of the Former Arid Zones of Zimbabwe, Zambia and Angola. *Transactions of the Institute of British Geographers,* 9**,** 75-88.

Thomas, D. S. G., G. Brook, P. Shaw, M. Bateman, K. Haberyan, C. Appleton, D. Nash, S. McLaren & F. Davies (2003) Late Pleistocene wetting and drying in the NW Kalahari: an integrated study from the Tsodilo Hills, Botswana. *Quaternary International,* 104**,** 53-67.

Thomas, D. S. G. & H. C. Leason (2005) Dunefield activity response to climate variability in the southwest Kalahari. *Geomorphology,* 64**,** 117-132.

Thomas, D. S. G., D. J. Nash, P. A. Shaw & C. Van der Post (1993) Present day lunette sediment cycling at Witpan in the arid southwestern Kalahari Desert. *CATENA,* 20**,** 515-527.

Thomas, D. S. G. & P. A. Shaw (1990) The deposition and development of the Kalahari Group sediments, Central Southern Africa. *Journal of African Earth Sciences,* 10**,** 187-197.

Thomas, D. S. G. & P. A. Shaw (2002) Late Quaternary etnvironmental change in central southern Africa: new data, synthesis, issues and prospects. *Quaternary Science Reviews,* 21**,** 783-797.

Tyson, P. D. & R. A. Preston-Whyte. 2000. *The weather and climate of southern Africa*. Cape Town; New York: Oxford University Press.

Wintle, A. G. (2006) A review of quartz optically stimulated luminescence characteristics and their relevance in single-aliquot regeneration dating protocols. *Radiation measurements,* 41**,** 369.

Wright, E. P. (1978) Geological Studies in the Northern Kalahari. *The Geographical Journal*, 144**,** 235-249.

Appendix A: Grain size analysis data.

		phi interval (weight in grams)												
	Depth (m)	**-0.5**	**0**	**0.5**	**1**	**1.5**	**2**	**2.5**	**3**	**3.5**	**4**	**Silt**	**Clay**	**total**
Linear Dune (MURU-6)	0	0.00	0.04	0.23	3.20	6.51	5.92	4.29	4.49	2.06	1.48	1.19	0.76	30.17
	0.5	0.00	0.03	0.23	2.35	5.30	5.24	3.89	4.39	2.71	1.25	1.24	0.92	27.56
	1	0.02	0.03	0.24	2.04	3.97	4.80	4.41	5.02	3.01	1.41	1.17	0.76	26.88
	2	0.00	0.02	0.19	1.24	2.63	2.90	2.87	3.35	2.07	1.04	0.65	0.67	17.64
	3	0.00	0.00	0.29	1.70	2.95	3.22	3.59	4.34	2.82	1.35	1.14	0.62	22.02
	3.3	0.07	0.08	0.36	2.32	4.17	4.79	4.74	4.27	3.33	1.51	1.86	1.03	28.53
Average		**0.02**	**0.03**	**0.26**	**2.14**	**4.26**	**4.48**	**3.97**	**4.31**	**2.67**	**1.34**	**1.21**	**0.80**	
Outer Lunette (MURU-19)	0	0.00	0.01	0.02	0.45	2.65	6.28	4.51	3.51	1.65	0.62	0.44	0.30	20.44
	0.5	0.00	0.00	0.05	0.53	2.29	5.64	5.24	5.20	2.84	1.18	0.83	0.69	24.49
	1	0.00	0.00	0.01	0.42	2.13	5.25	5.28	5.43	2.92	1.07	0.81	0.69	24.01
	2	0.00	0.00	0.04	0.54	2.36	5.71	6.71	7.20	3.91	1.62	0.99	0.96	30.04
	3	0.00	0.00	0.04	0.41	1.46	3.42	4.48	4.98	2.38	1.10	1.32	0.69	20.28
	4	0.00	0.00	0.06	0.51	1.82	4.73	6.37	7.13	3.84	1.25	1.04	0.50	27.25
	4.75	0.00	0.00	0.06	0.48	1.59	3.93	5.04	5.08	2.57	0.96	0.63	0.58	20.92
	5	0.00	0.01	0.11	0.81	2.47	5.53	6.85	6.99	3.56	1.25	1.10	1.01	29.69
Average		**0.00**	**0.00**	**0.05**	**0.52**	**2.10**	**5.06**	**5.56**	**5.69**	**2.96**	**1.13**	**0.90**	**0.68**	
Inner Lunette (MURU-3)	0	0.00	0.00	0.24	1.86	4.52	5.86	5.07	5.90	3.16	1.02	1.53	0.86	30.02
	0.5	0.00	0.02	0.19	1.28	3.01	4.04	4.21	4.99	2.85	1.13	1.37	1.65	24.74
	2	0.00	0.03	0.13	0.97	2.52	3.28	3.40	3.93	2.31	0.91	1.12	1.84	20.44
	3	0.00	0.06	0.18	1.25	3.01	3.82	3.76	4.18	2.26	0.81	1.26	2.10	22.69
	4.1	0.01	0.00	0.17	1.03	2.47	3.01	3.03	3.42	1.88	0.64	1.00	1.85	18.51
Average		**0.00**	**0.02**	**0.18**	**1.28**	**3.11**	**4.00**	**3.89**	**4.48**	**2.49**	**0.90**	**1.26**	**1.66**	
Shore Ridge (MURU-15)	0	0.01	0.06	0.38	2.46	2.70	3.69	3.21	4.32	2.63	0.87	1.25	2.09	23.67
	0.5	0.00	0.05	0.16	0.81	2.41	4.16	4.99	7.41	4.75	1.83	1.71	2.40	30.68
	1.1	0.00	0.01	0.13	0.55	1.54	3.05	3.63	5.48	3.54	1.28	1.22	1.56	21.99
	2	0.00	0.08	0.41	1.02	1.74	2.88	3.69	5.30	3.56	1.53	2.22	2.38	24.80
	2.5	0.02	0.10	0.33	0.76	1.50	2.41	3.00	4.13	2.64	1.03	1.61	2.64	20.17
Average		**0.01**	**0.06**	**0.28**	**1.12**	**1.98**	**3.24**	**3.70**	**5.33**	**3.42**	**1.31**	**1.60**	**2.21**	

		phi interval (%)												
	Depth (m)	**-0.5**	**0**	**0.5**	**1**	**1.5**	**2**	**2.5**	**3**	**3.5**	**4**	**Silt**	**Clay**	**Total**
Linear Dune (MURU-6)	0	0.00	0.13	0.76	10.61	21.58	19.62	14.22	14.88	6.83	4.91	3.94	2.53	100.00
	0.5	0.00	0.11	0.83	8.53	19.23	19.01	14.11	15.93	9.83	4.54	4.52	3.36	100.00
	1	0.07	0.11	0.89	7.59	14.77	17.86	16.41	18.68	11.20	5.25	4.34	2.84	100.00
	2	0.00	0.11	1.08	7.03	14.91	16.44	16.27	18.99	11.73	5.90	3.71	3.83	100.00
	3	0.00	0.00	1.32	7.72	13.40	14.62	16.30	19.71	12.81	6.13	5.15	2.84	100.00
	3.3	0.25	0.28	1.26	8.13	14.62	16.79	16.61	14.97	11.67	5.29	6.54	3.59	100.00
Average		**0.05**	**0.12**	**1.02**	**8.27**	**16.42**	**17.39**	**15.65**	**17.19**	**10.68**	**5.33**	**4.70**	**3.16**	
Outer Lunette (MURU-19)	0	0.00	0.05	0.10	2.20	12.96	30.72	22.06	17.17	8.07	3.03	2.15	1.47	100.00
	0.5	0.00	0.00	0.20	2.16	9.35	23.03	21.40	21.23	11.60	4.82	3.40	2.81	100.00
	1	0.00	0.00	0.04	1.75	8.87	21.87	21.99	22.62	12.16	4.46	3.38	2.86	100.00
	2	0.00	0.00	0.13	1.80	7.86	19.01	22.34	23.97	13.02	5.39	3.29	3.20	100.00
	3	0.00	0.00	0.20	2.02	7.20	16.86	22.09	24.56	11.74	5.42	6.52	3.39	100.00
	4	0.00	0.00	0.22	1.87	6.68	17.36	23.38	26.17	14.09	4.59	3.82	1.83	100.00
	4.75	0.00	0.00	0.29	2.29	7.60	18.79	24.09	24.28	12.28	4.59	3.04	2.75	100.00
	5	0.00	0.03	0.37	2.73	8.32	18.63	23.07	23.54	11.99	4.21	3.70	3.41	100.00
Average		**0.00**	**0.01**	**0.19**	**2.10**	**8.61**	**20.78**	**22.55**	**22.94**	**11.87**	**4.56**	**3.66**	**2.72**	
Inner Lunette (MURU-3)	0	0.00	0.00	0.80	6.20	15.06	19.52	16.89	19.65	10.53	3.40	5.09	2.87	100.00
	0.5	0.00	0.08	0.77	5.17	12.17	16.33	17.02	20.17	11.52	4.57	5.54	6.67	100.00
	2	0.00	0.15	0.64	4.75	12.33	16.05	16.63	19.23	11.30	4.45	5.49	8.99	100.00
	3	0.00	0.26	0.79	5.51	13.27	16.84	16.57	18.42	9.96	3.57	5.55	9.26	100.00
	4.1	0.05	0.00	0.92	5.56	13.34	16.26	16.37	18.48	10.16	3.46	5.40	9.99	100.00
Average		**0.01**	**0.10**	**0.78**	**5.44**	**13.23**	**17.00**	**16.70**	**19.19**	**10.69**	**3.89**	**5.41**	**7.56**	
Shore Ridge (MURU-15)	0	0.04	0.25	1.61	10.39	11.41	15.59	13.56	18.25	11.11	3.68	5.29	8.82	100.00
	0.5	0.00	0.16	0.52	2.64	7.86	13.56	16.26	24.15	15.48	5.96	5.57	7.82	100.00
	1.1	0.00	0.05	0.59	2.50	7.00	13.87	16.51	24.92	16.10	5.82	5.54	7.11	100.00
	2	0.00	0.32	1.65	4.11	7.02	11.61	14.88	21.37	14.35	6.17	8.93	9.58	100.00
	2.5	0.10	0.50	1.64	3.77	7.44	11.95	14.87	20.48	13.09	5.11	7.99	13.08	100.00
Average		**0.03**	**0.26**	**1.20**	**4.68**	**8.14**	**13.32**	**15.22**	**21.83**	**14.03**	**5.35**	**6.67**	**9.28**	